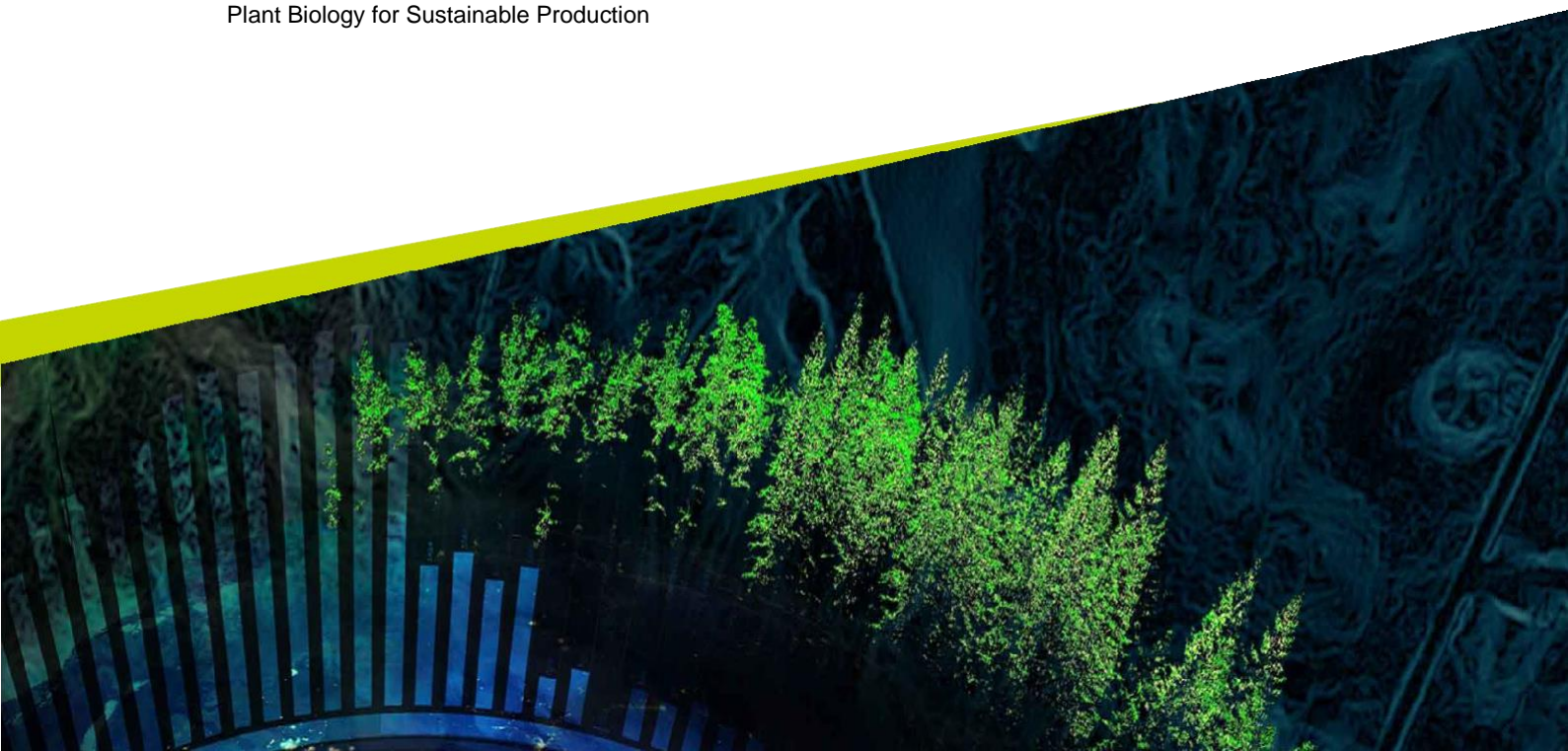




Investigating the role of a putative peptidase inhibitor in *Verticillium* species virulence.

Vilda Lindberg

Degree project • 30 credits
Swedish University of Agricultural Sciences, SLU
Department of Forest Mycology and Plant Pathology
Plant Biology for Sustainable Production



Investigating the role of a putative peptidase inhibitor in *Verticillium* species virulence.

Vilda Lindberg

Supervisor: Georgios Tzelepis, SLU, Department of Forest Mycology and Plant Pathology

Assistant supervisor: Magnus Karlsson, SLU, Department of Forest Mycology and Plant Pathology

Assistant supervisor: Anastasios Samaras, SLU, Department of Forest Mycology and Plant Pathology

Assistant supervisor: Vahideh Rafiei, SLU, Department of Forest Mycology and Plant Pathology

Examiner: Anna Berlin, SLU, Department of Forest Mycology and Plant Pathology

Credits: 30 credits

Level: Course, Second-cycle

Course title: Master thesis in Biology, A2E

Course code: EX0895

Programme/education: Abiotic and Biotic Interactions of Cultivated Plants - ODLA

Place of publication: Uppsala

Year of publication: 2024

Copyright: All featured images are used with permission from the copyright owner.

Keywords: *Verticillium*, *Verticillium longisporum*, *Verticillium dahliae*, plant peptidase inhibitors.

Swedish University of Agricultural Sciences
Department of Forest Mycology and Plant Pathology

Abstract

Peptidase inhibitors are released by fungal pathogens in order to inhibit peptidase activity against fungal effectors or metabolites during infection. *VL3320* is a putative peptidase inhibitor found in *V. longisporum* belonging to the I78 family of peptidase inhibitors. *VD3424* is a homolog of *VL3320* found in *V. dahliae* which present very similar functions and induction patterns. Through phylogenetic analysis, the I78 signal peptide domain as well as the potential catalytic region appeared to be conserved among all homologs identified. Both *VD3424* and *VL3320* showed low signs of upregulation until 5 days post inoculation, from which the genes were then downregulated until very low levels of expression at 8 days post inoculation. The homolog *VD3424* is shown to interact with the pathosystem of *Nicotiana benthamiana*, upregulating PR proteins and transcription factor *PR1*, *PTI5*, and *WRKY7*. Conversely, there appears to be a suppression of *HIN1* and *MAPKKKa*, and further analysis could determine whether *VL3320* is able to suppress proteins or transcription factors involved in the hypersensitive response and programmed cell death molecular pathways. In conclusion, *VL3320* is involved in infection and elicits plant immune responses upon infection of *V. longisporum*, further analytical steps will highlight specific mechanisms of *VL3320* in infection.

Table of contents

List of tables	6
List of figures.....	7
1. Introduction	10
1.1 <i>Verticillium longisporum</i> and <i>Verticillium dahlia</i>	10
1.1.1 <i>Verticillium longisporum</i>	10
1.1.2 <i>Verticillium dahliae</i>	11
1.1.3 Infection Process and Disease Cycle.....	11
1.1.4 Symptoms	12
1.2 Effectors from Plant Pathogenic Fungi	13
1.3 Fungal Peptidase Inhibitors	14
1.4 Hypothesis and Aims.....	15
2. Materials and Methods.....	16
2.1 Phylogeny.....	16
2.2 Functional Analysis.....	16
2.2.1 Fungal isolate and inoculum preparation.....	16
2.2.2 <i>In vitro</i> growth of tomato seedlings and inoculation.....	16
2.2.3 RNA extraction	17
2.2.4 Transcription analysis.....	18
2.2.5 Construction of deletion cassette	18
2.2.6 Protoplast Transformation	19
2.3 Transient expression of VL3320 in plants	21
2.3.1 Production of overexpression construct	21
2.3.2 <i>Agrobacterium</i> Mediated Transformation	24
2.3.3 PCR Validation.....	25
2.3.4 Confocal Microscopy	25
2.4 Transcription analysis of host immunity marker genes.....	25
2.5 Hypersensitive Response Induction	26
3. Results	28
3.1 Genome Analysis and Phylogeny of Peptidase Inhibitors	28
3.2 Gene Expression Analysis of VL3320 and VD3424 <i>in planta</i>	32
3.3 Construction of <i>V. dahliae</i> deletion strain	33
3.4 VL3320 Transient Expression in plants.....	33
3.4.1 Confocal Microscopy of 506 Construct and Free GFP Construct	33

3.4.2 Gene Expression Analysis of in <i>Nicotiana benthamiana</i>	34
4. Discussion	36
4.1 Gene Expression of VD3424 and VL3320	36
4.2 Transient Expression of VL3320	36
4.3 Gene Deletion of VD3424	38
4.3.1 Subcellular Localisation of pgWB506VL3320	39
5. Conclusion.....	40
References	41

List of tables

Table 1. Primers used for the construction of VD3424 deletion cassette.....	18
Table 2: Visualisation of the deletion plate as well as controls, denoting the contents and whether a hygromycin overlay was added.	20
Table 3. Primers used and respective candidate gene targets in PCR, Gateway II Cloning, mutant validation for VL3320.....	22
Table 3. Primers used and respective candidate gene targets in qPCR for the identification of PR protein expression in transformed <i>Nicotiana benthamiana</i>	26
Table 4: Analysis of taxonomic groups where the I78 peptidase inhibit was present after blasting the VL3320 gene against them using Mycosm.....	29

List of figures

Fig.1. The disease cycle of <i>Verticillium longisporum</i> in oilseed rape. A. An oilseed rape plant infected with <i>V. longisporum</i> during the growing season where no major symptoms are seen. B. Dark unilateral striping of microsclerotia. C. Plant debris decomposes. D. Microsclerotia from plant debris is released into the soil. E. Microsclerotia are triggered by root exudates and hyphae grow towards the roots of the plant. F. Hyphae enter root cells and release conidia. Created using BioRender.....	12
Fig. 2. Symptoms of <i>V. longisporum</i> . Left: infected with <i>V. longisporum</i> Right: control (photo by Marion Orsucci).....	13
Fig. 3: Seedlings of rapeseed cultivar “Hannah” being inoculated in the <i>V. longisporum</i> conidia suspension by the root-dip method.....	17
Fig. 5: Microscopy image taken on (microscope name and cam) detailing the validation of protoplast presence in the suspension, also including smaller conidia which passed through the filter.....	20
Fig. 4: Deletion cassette visualised using SnapGene	21
Fig. 6: VL3320pDONOR destination vector for the Gateway II cloning BP reaction visualised in SnapGene	23
Fig. 7: VL3320pGWB506 construct for <i>Agrobacterium</i> -mediated transformation in <i>Nicotiana benthamiana</i> with eGFP and VL3320 gene visualised in SnapGene	23
Fig. 8: VL3320pGWB602 construct for <i>Agrobacterium</i> -mediated transformation into <i>Nicotiana benthamiana</i> without GFP labelling visualised in SnapGene.....	24
Figure. 9: SMART analysis results identifying the presence of the inhibitor I78 from analysis of the VL3320 gene.....	28
Figure. 10: Molecular Phylogenetic analysis of genes found by MycoCosm with the I78 peptidase inhibitor present using the Maximum Likelihood method based on Whelan and Goldman model. Highlighted genes denote the genes of interest analysed from <i>V. longisporum</i> and <i>V. dahlia</i>	29
Fig. 11: A sequence logo denoting the sequence conservation of the homologs containing the I78 peptidase inhibitor region of VL3320. Made using WebLogo (Crooks et al., 2004) Each logo consists of stacks of symbols, one stack for each position in the sequence. The overall height of the stack indicates the sequence conservation at that position, while the height of symbols within the stack indicates the relative frequency of each amino acid at that position.	31
Fig. 12: Gene expression of VD3424 in <i>Solanum lycopersicum</i> variety ‘Moneymaker’ at mycelial stage, 2, 5, 8, and 9 days post infection with <i>Verticillium dahliae</i> isolate JR2.	32

Fig. 13: Gene expression of VL3320 in Brassica napus variety ‘Hannah’ at mycelial stage, 2, 4, 6, 8 and 10 days post infection with Verticillium longisporum isolate VL-1.....33

Fig. 14: Zeiss confocal laser scanning microscope LSM800 showing microscopy of leaf expressing free GFP construct in Nicotiana benthamiana.....34

Fig. 15: Graphs detailing the gene expression. Y axis denotes to the RT-qPCR Ct values normalised against Nicotiana benthamiana 18S gene expression after infecting with VL3320pgWB602. Corresponding letters denote no significant difference between each other (p-value >0.05) while differing letters corresponds to a significant difference (p-value: ≤0.05)35

Abbreviations

VD3424	VDAG_00003424
VL3320	VL_T00003320
602	pGWB602
506	pGWB506

1. Introduction

Fungal infections of agricultural crops reduce total worldwide yield by 10-23 percent per year (Steinberg and Gurr, 2020). This significant loss threatens global food security and emphasizes the importance in understanding molecular mechanisms behind fungal virulence for the production of tolerant or resistant crops. Oilseed rape (*Brassica napus*) is a major economically important crop in the EU and Sweden and is the second most important oil crop after soybean (Eurostat, 2022). Since 2001, the production of rape seeds has increased significantly by almost 200% (Eurostat, 2022), due to its use for both animal feed, human consumption and biodiesel. Efforts towards understanding the infection biology of pathogens associated with yield losses have become pertinent due to its increasing value. *Verticillium* is a genus of soil-borne ascomycete fungi comprised of 10 species infecting mostly brassicaceous and solanaceous hosts. *Verticillium longisporum* is a monocyclic soil-borne fungus, that infects the vasculature of Brassica plants, and has a disease incidence rate of up to 80% with a yield loss of up to 50% in Europe (Dunker et al., 2008). It can infect not only brassicaceous plants, but also eggplant, tomato and watermelon and is the most economically important disease affecting oilseed rape (Novakazi et al., 2015). *Verticillium longisporum* is an emerging pathogen found in Sweden (Tzelepis et al., 2017), England (Depotter et al., 2017), Canada (Heale and Karapapa, 1999), Japan (Banno et al., 2011) and other countries, infecting *Brassicaceous* hosts.

Species of plants in the genus *Brassica* are composed of several major economically important crops, many of which are grown for the production of oilseeds used for animal feed, human consumption and biodiesel production. Due to the increasing value of oilseed crops, an understanding of the molecular mechanisms surrounding their infection is pertinent to creating crops with more durable resistance to these pathogens. In this thesis, a putative peptidase inhibitor gene in *V. longisporum*, also present as a homolog in the parental species *V. dahliae*, are studied to investigate their role in virulence.

1.1 *Verticillium longisporum* and *Verticillium dahliae*

1.1.1 *Verticillium longisporum*

Verticillium longisporum infects the vasculature of Brassica plants. In Sweden, the production of oilseed rape (*Brassica napus*) and turnip rape, two oilseed crops, are often infected by two pathogens, *Verticillium dahliae* causing Verticillium wilt and *Verticillium longisporum* causing Verticillium stem striping. *Verticillium longisporum* was previously thought to be a variation

of *V. dahliae*, named *V. dahliae* var. *longisporum*, and was raised to a species rank in 1997 (Karapapa, Bainbridge and Heale, 1997). The disease *V. longisporum* causes is also referred to in the literature as Verticillium wilt, however due to the differing symptoms between Verticillium wilt observed in *V. dahliae* infection and in *V. longisporum* infection, it will be referred in this study as Verticillium stem striping as described in previous literature (Depotter *et al.*, 2016).

Typically, ascomycetes live predominantly in the haploid stage, *V. longisporum*, however, is a result of hybridization between two haploid ancestors and therefore lives as an amphidiploid, having inherited a diploid set of chromosomes from each parent, with A1/D1 being the most virulent on oilseed rape (Vega-Marin and Von Tiedemann, 2023). Phylogenetic analyses separate three lineages of *V. longisporum* with four different parental lines: A1 and D1, unknown progenitors provisionally named haploid *Verticillium* species, and D2 and D3, *V. dahliae* lineages.

1.1.2 *Verticillium dahliae*

V. dahliae, a soil-borne hemibiotrophic pathogen belonging to the phylum Ascomycota, is a much more studied and understood species of *Verticillium* than *V. longisporum*. It has a larger host range than *V. longisporum*, being able to infect 200 crops and not only Brassicaceous hosts but also Solanaceous such as tomato and potato, fruits such as strawberry and melon; fibre crops such as cotton; perennials; and woody plants such as olive, peach and almond trees (Fradin and Thomma, 2006). Unlike *V. longisporum*, *V. dahliae* causes Verticillium wilt, a disease characterised by wilting, chlorosis and vein clearing due to the growth of the pathogen in vascular tissues leading to blockages in xylem transport (Zhang *et al.*, 2022).

1.1.3 Infection Process and Disease Cycle

The disease cycle of *V. longisporum* can be divided into two phases, the first being as an intracellular endophyte (Zhou *et al.*, 2006). *V. longisporum* overwinters and survives in soil as microsclerotia – cells derived from hyphae of the lateral budding of hyaline mycelium that are produced in the dying part of a plant. Microsclerotia are thick-walled fungal structures and have been noted to be able to survive for up to 14 years in the parent species *Verticillium dahliae* in the absence of a host, and possibly is similar to the resting period in *V. longisporum*. The germination of microsclerotia is dependent on contact with root exudates of the host plant which then stimulates the growth of hyphae towards the plant roots (Depotter *et al.*, 2016). The hyphae can enter the roots by wounds or direct penetration of the epidermal cells, and subsequently enter the xylem through intercellular and intracellular growth towards the cortex and vascular cylinder. Some studies have suggested the possibility of seed-borne infection of *V. longisporum* in seeds produced by significantly diseased oilseed rape plants (Zheng *et al.*, 2019)

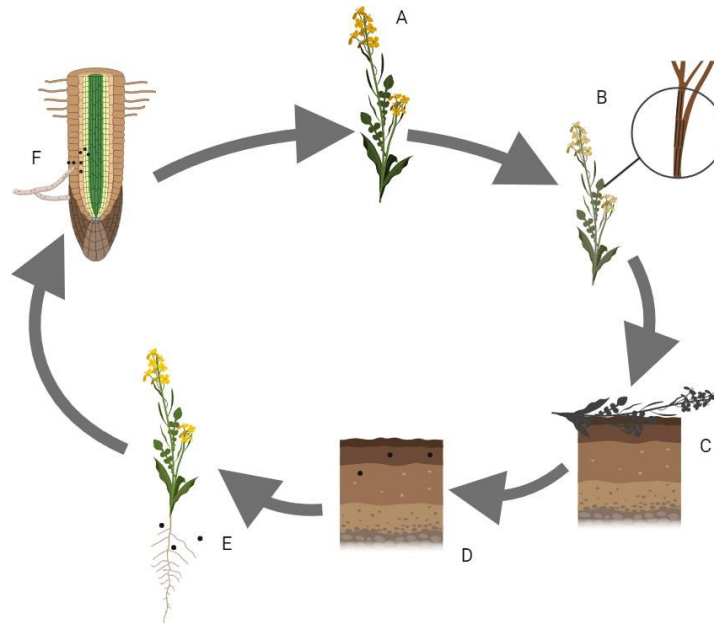


Fig.1. The disease cycle of *Verticillium longisporum* in oilseed rape. A. An oilseed rape plant infected with *V. longisporum* during the growing season where no major symptoms are seen. B. Dark unilateral striping of microsclerotia. C. Plant debris decomposes. D. Microsclerotia from plant debris is released into the soil. E. Microsclerotia are triggered by root exudates and hyphae grow towards the roots of the plant. F. Hyphae enter root cells and release conidia. Created using BioRender.

The second stage of *V. longisporum* infection is denoted as the period of hyphal proliferation and conidia production, wherein the conidia germinate and colonize the vascular elements upstream of the stem. The leaves senesce, and the conidia spread to the non-vascular elements of the plant, eventually colonizing the entire plant, while new microsclerotia are produced in dying leaves and mainly in the stems. The microsclerotia then remain in the soil when the plant debris falls off to the soil (Depotter et al., 2016).

At 14 days post infection, plants infected with *V. longisporum* begin to display chlorosis, at 21 days are visibly stunted and show infection symptoms on 20-50% of the leaves, beginning to show severe disease symptoms at around 35 days post infection (Eynck et al., 2007).

1.1.4 Symptoms

In oilseed rape, the symptoms of *V. longisporum* infection presents itself as dark unilateral striping along the stem due to necrosis of the root and stem colonization of the vascular systems. At the final stages of the disease cycle, black microsclerotia are formed in the stem cortex. The oilseed rape plant is significantly stunted due to the infection, ripening prematurely, and undergoing senescence which makes the disease hard to distinguish until the later stages where the microsclerotia are visible. The growth of the overall plant is clearly reduced, significantly in the roots which are the most affected plant parts.

In most other brassicaceous hosts, *V. longisporum* displays clear symptoms of the Verticillium wilt disease, predominantly categorized by initial chlorosis and wilting of the lower older leaves, and later, stunting, entire plant wilt, and areas of necrosis. In broccoli however, *V. longisporum* is not able to colonize the vascular system and produce disease

symptoms of *Verticillium* wilt, which may be attributed to the high concentration of aliphatic glucosinolates in the root system of broccoli after infection (Njoroge *et al.*, 2011)



Fig. 2. Symptoms of *V. longisporum*. Left: infected with *V. longisporum* Right: control (photo by Marion Orsucci)

1.2 Effectors from Plant Pathogenic Fungi

Compatible interactions between a plant infecting fungus and a host are determined by the specificity of the fungal effectors (Lo Presti *et al.*, 2015). Effectors are molecules that can differ in function but are ultimately secreted by the fungus in order to promote colonisation and growth of the fungus in the host.

Plants have highly specialised defence systems to determine and produce immune responses against pathogen attacks. The first line of defence for plants is its passive defences, such as lignin, cutin, and preformed chemical defences on the plant barrier whose expression is not elicited by the presence of a pathogen or herbivore.

Pattern recognition receptors, or PRRs, are the cell surface receptors receptor-like kinases (RLK) and receptor-like proteins (RLP) which trigger pattern-triggered immunity (PTI), commonly referred to as the second line of defence. PTI is triggered upon the recognition of pathogen-associated microbial patterns (PAMPs) or damage-associated microbial patterns (DAMPs). One example of a common fungal PAMP is chitin, the major cell wall component of fungi. In *Arabidopsis thaliana*, *CERK1* is an RLK which elicits an immune response following the recognition of the chitin oligosaccharide (Zipfel, 2008).

Effector-triggered immunity (ETI) is another subclass linked to PTI (Yuan *et al.*, 2021) immunity in which the recognition of effectors by Nucleotide Binding – Leucine Rich Repeats (NB-LRRs) induces an immune response with more specificity to the infecting pathogen, and

ETI responses in some cases require pairs of NB-LRRs for the recognition of an effector (Eitas and Dangl, 2010).

Fungi are often grouped into three lifestyles depending on their mode of infection: biotrophic, hemibiotrophic and necrotrophic, with effector functions specific to their mode of infection. Biotrophic fungi, for example, require a living host and effectors that are able to suppress host immunity such as metabolic pathways that induce plant cell death, such as the induction of reactive oxygen species (ROS), while necrotrophic pathogens secrete effectors that induce these pathways. A biotrophic pathogen, *Ustilago maydis*, secretes the effector *TIN2* which prevents the lignification of plant cell walls and allows the fungus to colonise neighbouring cells more easily (Tanaka *et al.*, 2014). As *V. longisporum* is a hemibiotrophic pathogen, the effectors released initially are biotrophic and pertain to dampening the plant defence system, and later during the necrotrophic stage the effectors released are to induce plant cell death (Depotter *et al.*, 2016).

Many effectors are transferred into the genomes of other pathogens, in an event known as horizontal gene transfer. In *V. dahliae*, a proposed 42 effectors are known to be present in the genome from bacterial donors (Shi-Kunne *et al.*, 2019).

1.3 Fungal Peptidase Inhibitors

Proteolytic enzymes are enzymes that have a range of functions in both primary and secondary metabolism in plants, as well as in pathogen defence (Fernández-Fernández, Stael and Van Breusegem, 2023). Proteases are essential to plant growth in metabolic processes such as nitrogen metabolism, signal transduction, fate determination of proteins but are also important in pathogen defence, often used to cleave protein products of pathogens that are significant to the growth of the pathogen or infection of the plant (Sabotič and Kos, 2012).

Fungal peptidase inhibitors are released by fungal pathogens in order to inhibit peptidase activity against fungal effectors or metabolites during infection. The T-64 strain of *Aspergillus japonicus* for example, contains a protease inhibitor E-64 (Hanada *et al.*, 1978) with a specificity towards thiol proteases such as papain, notably important in plant growth due to its involvement in plant growth under stress conditions such as drought (Sharma and Gayen, 2021).

The *VL_T00003320* gene, denominated as *VL3320*, encodes a putative peptidase inhibitor in *V. longisporum*, and a homolog gene (*VDAG_00003424*) has also been identified in *V. dahliae* as well. Peptidases are catalytic enzymes involved in plant immunity that cleave or inhibit small peptides like pathogen-related proteins (PR proteins). Peptidase inhibitors are secreted as a ‘counterattack’ after PTI (PAMP-triggered immunity) in order to interfere with the enzymatic function of peptidases and have generally been found to have a remarkable specificity to peptidases, with studies suggesting that there is a co-evolutionary arms race in plant-pathogen adaptations of peptidase – peptidase inhibitor interactions (Hörger and Van Der Hoorn, 2013). Although the presence of other peptidase inhibitors in *V. longisporum* has been

identified, the molecular mechanisms in and of itself and in virulence are as of yet still unclear (Dunaevsky *et al.*, 2014).

1.4 Hypothesis and Aims

VL3320 is hypothesised to be involved in *Verticillium* virulence due to its potential role as a peptidase inhibitor. The aims of this study are as follows:

- To identify the role of *VL3320* in *Verticillium* virulence
- To understand the effect of *VL3320* on plant immunity

In order to achieve these aims, phylogenetic analysis was used to identify similar genes and narrow down its function, and functional analysis was used to more robustly recognise function by analysing the interaction of *VL3320* with specific plant defence genes as well as scrutiny of up or downregulation *in planta*. Due to the economic importance of several *Verticillium* hosts, and the unclarity of the function of *VL3320*, elucidating the potential role of *VL3320* as a peptidase inhibitor is critical to a deeper more fundamental understanding of *Verticillium longisporum* infection.

2. Materials and Methods

2.1 Phylogeny

The Mycosm database ([Mycosm \(doe.gov\)](http://mycosm.doe.gov)) was used to investigate whether the protein as well as the functional peptidase inhibitor domain was present in other fungal species. The homologs as well as the presence of the peptidase inhibitor were noted, and the sequences of the genes with the peptidase inhibitor present were aligned using MAFFT and used to construct a maximal phylogeny tree in MEGA 7. The evolutionary history was inferred by using the Maximum Likelihood method based on the Whelan and Goldman model (Whelan and Goldman, 2001). Evolutionary analyses were conducted in MEGA7 (Kumar, Stecher and Tamura, 2016). The domain structure of the protein was investigated using the SMART software (<http://smart.embl-heidelberg.de/>)

2.2 Functional Analysis

2.2.1 Fungal isolate and inoculum preparation

In inoculation, the *V. dahliae* strain JR2 and the *V. longisporum* strain VL1 were used due to their high virulence, as well as prevalence in literature (Rafiei *et al.*, 2022, Song and Thomma, 2016) and therefore broadest understanding. The strains were inoculated on PDA plates and left to grow in the darkness at 20°C for one week. The conidia were then harvested by adding 10ml of autoclaved water into the plate and scraping using a cell scraper. The conidia suspension was then poured into a beaker with a Miracloth filter and the concentration of the cell suspension was counted using a haemocytometer and adjusted to 10⁶.

2.2.2 *In vitro* growth of tomato seedlings and inoculation

Seeds of tomato cultivar “Moneymaker” and rapeseed seed from the cultivar “Hannah” were used for *in vitro* infection with *V. dahliae* and *V. longisporum* respectively. Surface sterilisation of seeds was performed by placing the seeds in 70% bleach for 1 minute before adding water to allow the seeds to sink. Bleach and water were drained, and 10% ethanol was added to the seeds and allowed to sit for 1 minute before being washed three times with water. Seeds were grown in half strength Murashige-Skoog medium and placed in a growth chamber at 22°C with

a 16-hour photoperiod. After one week, the seedlings were removed and infected by submerging the roots of the seedlings (root-dip method (Trapero *et al.*, 2013)) in the 10^6 -inoculum suspension for 15 minutes before being placed in new plates with half strength Murashige-Skoog without sucrose.



Fig. 3: Seedlings of rapeseed cultivar “Hannah” being inoculated in the *V. longisporum conidia* suspension by the root-dip method.

One plate was produced as a mock, and the seedlings were instead dipped in water for 15 minutes before being transferred to a new plate. The roots and stem of the seedlings were then harvested at 2-, 5-, 8- and 9-days post infection for the tomato plants, and harvested at 2-, 4-, 6- and 8-days post infection for the oilseed rape plants, washed in ethanol and rinsed in water to remove any mycelia from the outside of the seedling before being frozen in liquid nitrogen and mechanically ground using a mortar and pestle, stored in -80°C for RNA extraction. The mycelia of *V. dahliae* was also mechanically ground using liquid nitrogen and a mortar and pestle and stored in -80°C in order to measure gene expression of the target gene in mycelia.

2.2.3 RNA extraction

RNA extraction of the frozen samples was done using the Sigma Aldrich Plant Total RNA Kit following the manufacturers protocol and the quality was measured using a Bioanalyzer (Agilent Technology). The samples were then treated with DNase by Thermo Fisher Scientific following the manufacturers protocol and transcribed to cDNA using the iScript cDNA Synthesis Kit (Bio-Rad).

2.2.4 Transcription analysis

For transcription analysis of *Verticillium* peptidase inhibitor, each RT-qPCR reaction was performed in a total volume of 10 μ L with 5 μ L of EvaGreen MasterMix (Bio-Rad), 0.2 μ L of each primer, 2 μ L of DNA and 2.6 μ L of MilliQ water. Each reaction was performed in two technical and at least five biological replicates and using a 2-step melt amp protocol: 95°C for 15 minutes, 94°C for 10 seconds, 66°C annealing temperature for 30 seconds, and 72°C for 30 seconds. The RNA used was from the 2-, 5-, 8- and 9- day time point plants as well as mycelia harvested from JR2. The Ct values were normalised with the housekeeping gene GAPDH using the cDNA and 2x EvaGreen master mix with GAPDH primers (Table 1). Another RT-qPCR was then performed using the VDAG03424 primers (Table 1) for the *V. dahliae* infected samples in order to examine how gene expression of the target genes varied with days post infection. Relative expression values were calculated from the threshold cycle (Ct) values according to the $2^{-\Delta\Delta CT}$ method (Livak and Schmittgen, 2001). For VL1, the RNA used was from the 2-, 4-, 6-, and 8- day time point plants as well as mycelia harvested from VL1. GAPDH was also used for the normalization of the VL1 infected oilseed rape plants, and the VL3320 primers were used afterwards in order to examine how gene expression of the target genes varied with days post infection.

Table 1. Primers used for the construction of VD3424 deletion cassette. Primers provided by Georgios Tzelepis.

Gene	Oligo Name	Oligo Sequence
VD3424	VD3424upstream_FW	AATTCGAGCTCGGTACGGACGACCCATTGGC
VD3424	VD3424upstream_RV	TTGCGCGCGGTGTTTACTGTATGGC
VD3424	VD3424Hyg_F	TAAACACCGCGCGCAATTAACCC
VD3424	VD3424Hyg_R	TACCCCGCGAATTGCGCGTACAGA
VD3424	VD3424down_F	CGCAATTCGCGGGTATCGTCAT
VD3424	VD3424down_R	GCCAAGCTTGCATGCCGGTCTCCGCCGTGCC
GAPDH	GAPDH 5' – 3'	AGCTCAAGGGAATTCTCGATG/AACCTTAACC ATGTCATCTCCC

2.2.5 Construction of deletion cassette

Due to the amphidiploid nature of *V. longisporum*, the deletion of the VL3320 gene was instead performed in the *V. dahliae* homolog VDAG_00003424. For the construction of the deletion cassette the GeneArt™ Seamless Cloning technology (Invitrogen), was used according to manufacturer's instructions. Approximately 1000 bp upstream and downstream of VD3424 were amplified from *Verticillium dahliae* gDNA, using the high fidelity Phusion polymerase (98°C for 30 seconds, 98°C for 5 seconds, annealing at 65°C for 30 seconds, 72°C for 30

seconds, 72°C for 10 minutes). The bands were cut, and the gel was purified using the GeneJet Gel Extraction Kit (Thermo Fisher) following the manufacturer's protocol and ligated together with the hygromycin resistant gene to the pUC19 vector. The VD3424:pUC19 vector was transformed to OneShot™ *E. coli* TOP10 competent cells (Invitrogen). Two vials of competent cells were thawed on ice, one for the transformation of the VD3424 deletion cassette and one for the pUC19 control. 50ng of the deletion cassette was added to the competent cells and mixed gently. The pUC19 control instead had 1µl of pUC19 DNA added in order to ensure validity of the pUC19 vector itself. The vials were incubated on ice for 30 minutes, and heat shocked in a water bath at 42°C for 30 seconds and placed immediately on ice for 2 minutes. 250µl of warmed SOC media was added to the vials and the vials were placed in a shaking incubator horizontally for 2 hours at 37°C at 430rpm. After 2 hours, 200µl of both vials was spread onto a plate with LB media and 100ng ampicillin. The plates were closed with Micropore™ tape, inverted, and incubated at 37°C overnight.

2.2.6 Protoplast Transformation

Verticillium dahliae conidia harvested from PDA plates was grown in Potato-Dextrose Broth (PDB) for three days at 25°C with shaking to ensure mycelial growth in the broth. This mycelial suspension was then transferred to a 50ml conical tube and used to form protoplasts following an adapted version of a protocol for the transformation of filamentous fungi specifically *Botrytis cinerea*. The culture was harvested by centrifuging the suspension at 1500g for 8 minutes to pellet the mycelia and discarding the solute. To ensure all PDB was removed before protoplast transformation, the mycelia were washed in distilled water by adding 50ml distilled water and centrifuging before again discarding the solute. The mycelia were then washed in 25ml of OM buffer (1.2 M MgSO₄, 10mM Na-PO₄ at pH 5.8 diluted from 1.0 stock), centrifuged at the same conditions and the solute was discarded. 25ml of OM/500mg Glucanex (Invitrogen) was then added to the pellet and the hyphal clumps were dissolved by pipetting. The resulting solution was incubated at 30°C with gentle (70rpm) shaking for 2 hours. The protoplasts/OM buffer were filtered through Miracloth and transferred to a falcon tube. An equal volume cold TMS (54.66g of 0.6 M sorbitol, 50ml 1 M of 10mM Tris-HCL at pH 7.5, for 500ml) was added to the tube and spun in a swinging bucket rotor at 4000g/4°C for 5 minutes, and the solute was discarded. An equal volume TMSC (109.32g of 1.2M sorbitol, 5ml 1M of 10mM Tris-HCL at pH 7.5 10mM CaCl₂ for 500ml) was added to the protoplasts and the protoplasts were pelleted in the swinging bucket rotor with the same conditions, and the solute was discarded. The pellet was resuspended in 10ml of TMSC and the protoplasts were counted.

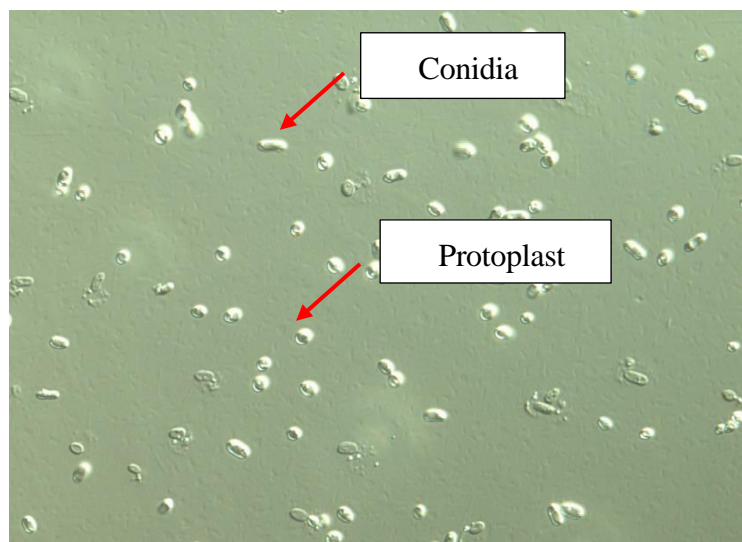


Fig. 5: Microscopy image taken on (microscope name and cam) detailing the validation of protoplast presence in the suspension, also including smaller conidia which passed through the filter.

The protoplasts were combined with 5 μ g of the deletion cassette VD3424 (VDAG_00003424) (figure 4) in 150ul of TMSO and incubated for 25 minutes at room temperature. 1ml of PTC (60g of 60% PEG 4000, 1ml 1 M of 10mM Tris HCl at pH 7.5, 1ml 1 M 10mM CaCl₂ for 100ml) was added and mixed gently by inversion and incubated for 20 minutes at room temperature.

The protoplasts were added to 150ml molten (42°C) agar medium (PDA/0.8M sucrose), mixed gently and poured into 2 50ml plates and 3 25ml plates. Two plates had the empty vector added instead of the construct as a positive control. The protoplasts were allowed to grow overnight before adding hygromycin in order to ensure higher success of the protoplasts incorporating the deletion of VD3424. After 16 hours of incubation at 20°C in the dark, 15ml of PDA/0.8M sucrose containing 50 μ g ml⁻¹ of hygromycin was overlaid onto 4 of 5 of the plates. One 25ml plate was overlaid with just PDA/0.8M sucrose without hygromycin as a living control.

Table 2: Visualisation of the deletion plate as well as controls, denoting the contents and whether a hygromycin overlay was added.

	Protoplast	Empty vector (pTel-Hyg)	Hygromycin (50 μ g ml ⁻¹)
Deletion	✓	✗	✓
Death Control	✗	✓	✓
Living Control	✓	✗	✗
Vector Control	✗	✓	✗

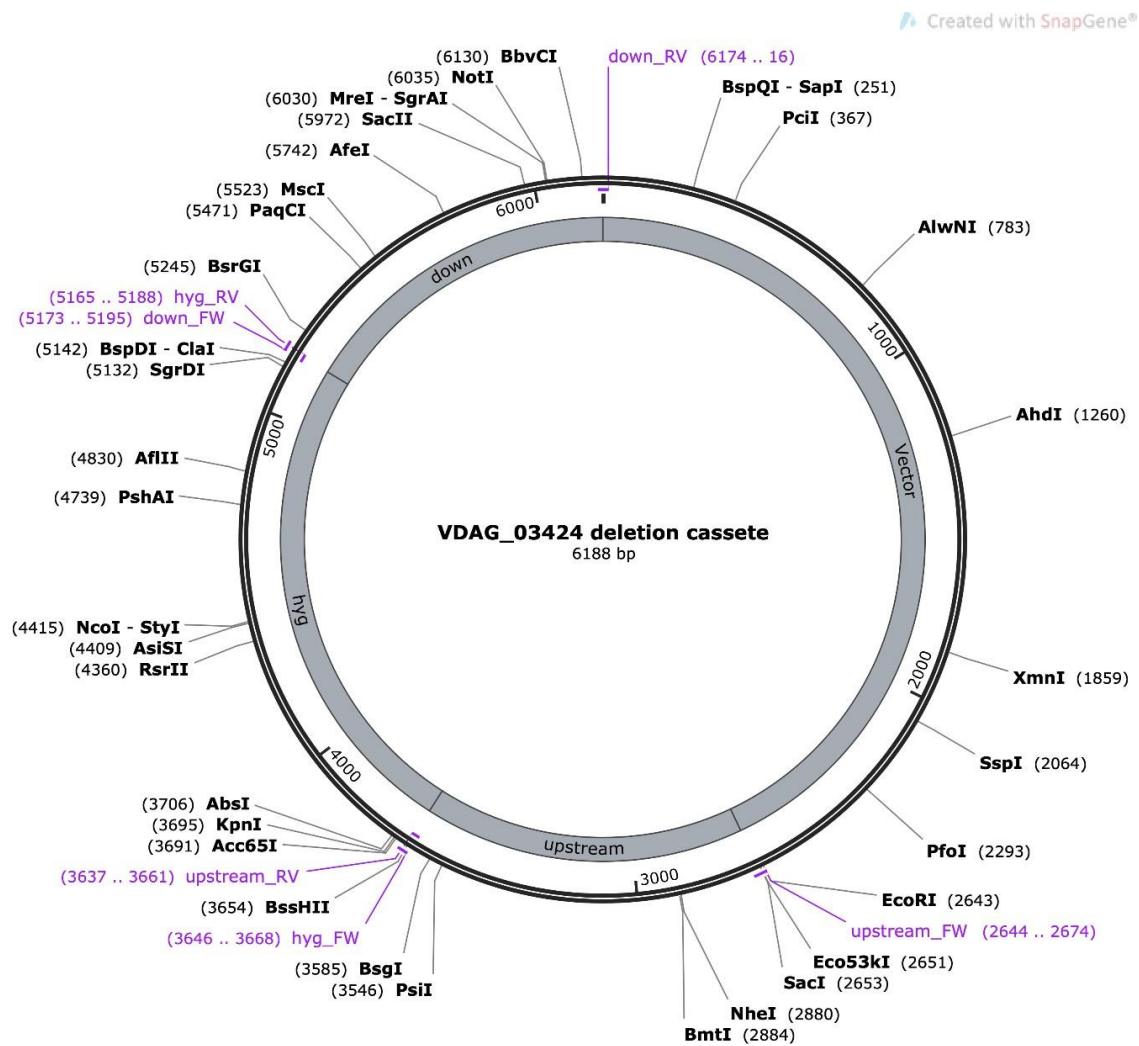


Fig. 4: Deletion cassette visualised using SnapGene

2.3 Transient expression of VL3320 in plants

2.3.1 Production of overexpression construct

The VL3320 gene was amplified through PCR by *V. longisporum* cDNA with DreamTaq PCR Master Mix (2X) (ThermoFisher), using pDONOR VL3320 primers (Table 2) following manufacturers protocols with conditions at 95°C for 3 minutes, 95°C for 30 seconds, 60°C for 30 seconds, 63°C annealing temperature for 1 minute, 72°C degrees for 5 mins. The PCR product was then purified by ethanol precipitation by adding 1 volume of water and 1 volume of chloroform to the PCR product and discarding everything but the upper phase. 1:10 volume of 3M sodium acetate was then added with 2.5 volumes 99% ethanol and incubated for 30 minutes at -80°C. After 30 minutes, the reaction was centrifuged for 20 minutes at 13000rpm,

and the pellet was washed with 100µl 70% ethanol. The product was centrifuged again at 13000 rpm for 5 minutes and dissolved in 50µl TE buffer (10mM Tris-HCl, 0.1mM EDTA). The presence of the gene was validated by sequencing.

The BP reaction was performed using Gateway® BP Clonase™ II Enzyme Mix (Invitrogen) following the manufacturers protocol, transformed to *E. coli* TOP10 cells, and the resulting entry clone VL3320: pDONR/Zeo (figure 6) was validated through restriction analysis using the Apal enzyme and sequencing. The LR reaction was performed using the Gateway™ LR Clonase™ II Enzyme Mix (Invitrogen) with the destination vector pGWB602 (figure 8), without any tag, and pGWB506 (Nakagawa et al., 2007), with GFP tag at N-terminus (figure 7), following the manufacturers protocol. The resulting reaction was plated on LB plates with spectinomycin, and the colonies were validated through sequencing and PCR.

Table 3. Primers used and respective candidate gene targets in PCR, Gateway II Cloning, mutant validation for VL3320

Candidate Gene	Oligo Name	Oligo Sequence 5' – 3'
VL3320	VDAG_03424pDONOR_F	GGGACAAGTTTGTACAAAAAAGCAG GCTTAATGTTGCATGCTTTCTGCTCAC T
VL3320	VDAG_03424pDONOR_R	GGGACCACTTTGTACAAGAAAGCTG GGTTTTATCCACGCTCGACGTGGG
VL3320	VL13320F	CAACCCCAACCTGCACCTCT
VL3320	VL13320R	TGCAGAAGCATGTCTCGTCGG
VL3320	VL3320_FW	CATCACCCATGTTGCATGCTTTCTG
VL3320	VL3320_RV	GTGGATAATGAGGACTTAATGGTGAG

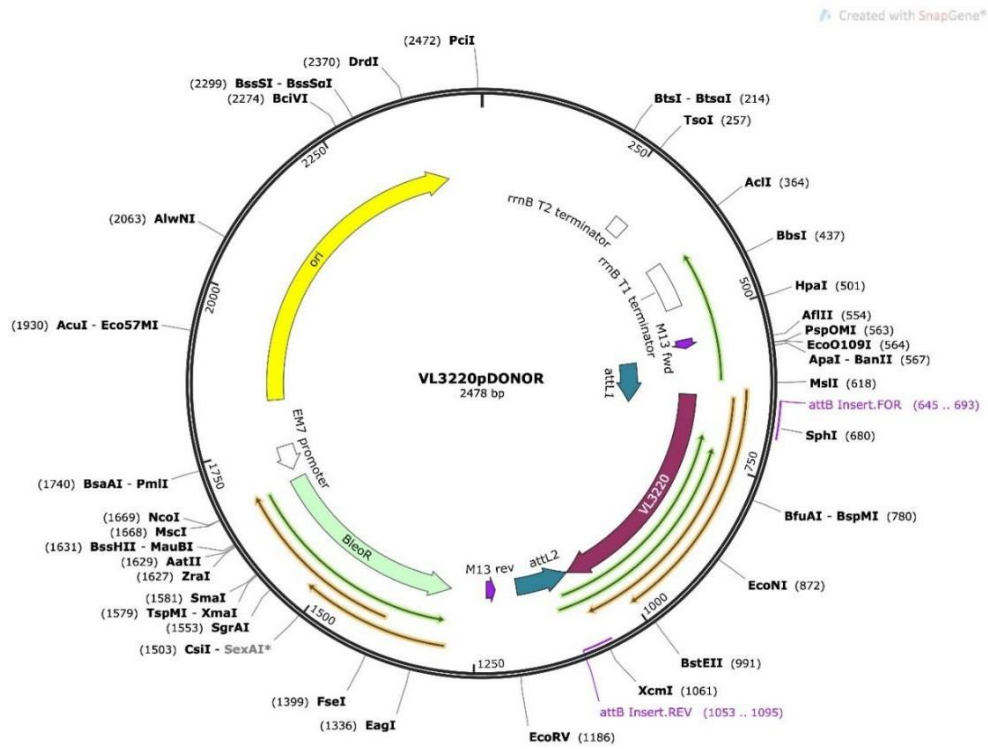


Fig. 6: VL3220pDONOR destination vector for the Gateway II cloning BP reaction visualised in SnapGene.

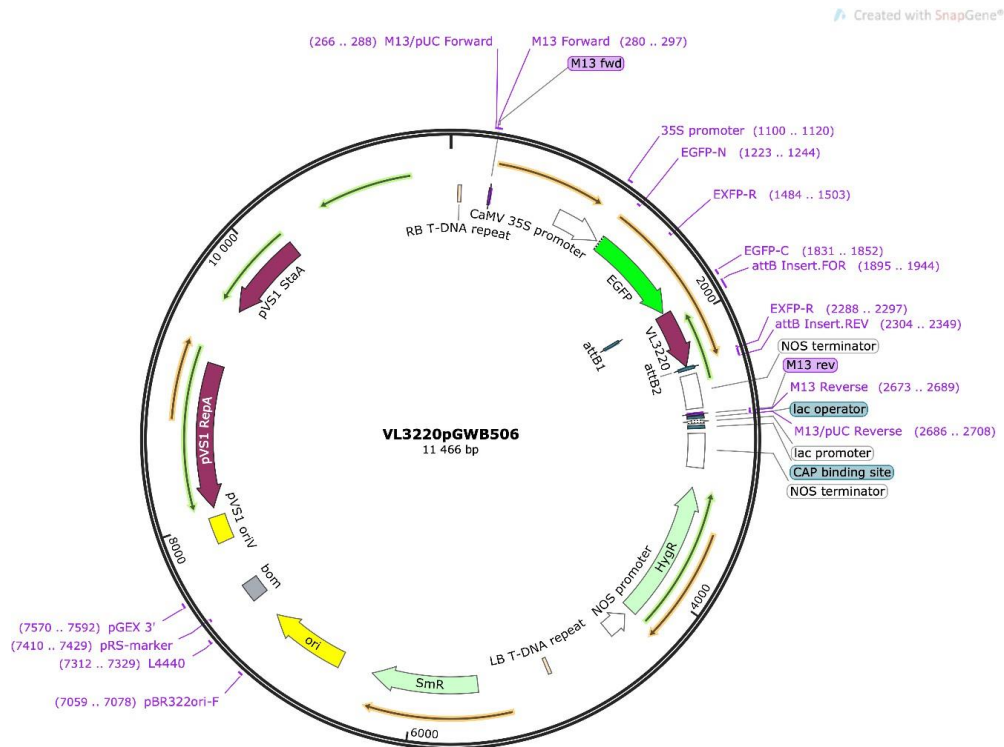


Fig. 7: VL3220pGWB506 construct for Agrobacterium-mediated transformation in *Nicotiana benthamiana* with eGFP and VL3220 gene visualised in SnapGene..

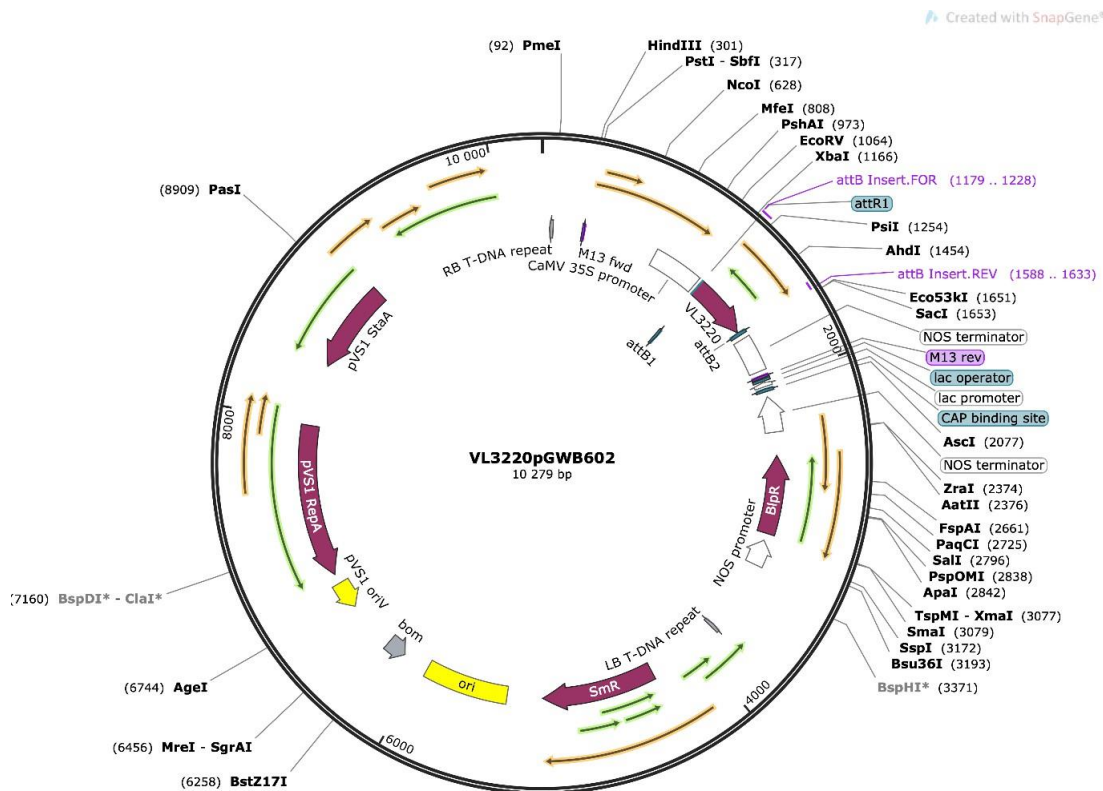


Fig. 8: VL3220pGWB602 construct for *Agrobacterium*-mediated transformation into *Nicotiana benthamiana* without GFP labelling visualised in SnapGene.

2.3.2 *Agrobacterium* Mediated Transformation

Two tubes of competent *agrobacterium* C58C1 cells were used to perform the transformation. The cells were thawed on ice and 5µl of the destination vectors (VL3220:pGWB602 and VL3220:pGWB506) was added to each tube of the thawed competent cells. The mixture was frozen in liquid nitrogen briefly before being transferred to a 37°C water bath for 5 minutes. 200µl of TSB media was added to the tube and the cells were left to grow for 3 hours at 28°C with shaking at 200rpm. The mixture was pelleted by spinning down in a centrifuge for 1 minute at 13000rpm and resuspended in 50µl LB. The resuspended cells were plated on selective LB (rafampicin and spectomycin) and grown for 2 days at 28°C. After 2 days, 4 colonies were isolated using a toothpick and dissolved into 10µl MilliQ water and were verified by PCR using the VDAG_03424pDONOR forward and reverse primers (table 2). 8µl of the colonies dissolved in water were transferred to a falcon tube with 40ml of LB media and 40µl of spectinomycin and put in a shaker at 28°C overnight.

The resuspended cells in the tube were then centrifuged at 3500rpm for 5 minutes at 4°C and the solute was discarded. The pellet was then dissolved in induction buffer containing 0.5M MES buffer (final concentration 10mM), 100mM acetosyringone (final concentration 150µM), 1M MgCl₂ (final concentration 10mM), and distilled water up to 100ml. This was then repeated, and the suspensions were then incubated in 28°C for two hours. Suspensions with free GFP and the empty vector were also treated in the same way used as controls. After two

hours, the OD of the cells was adjusted to 0.5 for constructs without GFP (VL3220:pGWB602, empty vector) and 0.2 for constructs with GFP (VL3220:pGWB506, free GFP).

The overexpression construct with GFP tagging (506) and the construct without GFP (602) was transformed into 4-week-old *Nicotiana benthamiana* plants by syringe infiltration. Three plants were infiltrated using a syringe with just induction buffer as a mock, and five were syringe infiltrated with the empty vector. The infiltrated area was outlined with a marker. The mock and first time point plants were harvested at 48- hours, while the second time point and plants infiltrated with the empty vector (EV) were harvested at 72-hours post infiltration, and the marked area was cut and mechanically ground in liquid nitrogen using a pestle and mortar and stored at -80°C. The plants with the expression of the VL3220:pGWB506 and free GFP construct were observed using confocal microscopy at 48 hours.

The RNA was extracted using the Sigma Aldrich Plant Total RNA Kit and was extracted following the manufacturers protocol and the quality was measured using a Bioanalyzer (Agilent Technology). The samples were then treated with DNase using Invitrogen by Thermo Fisher Scientific following the manufacturers protocol and transcribed to cDNA using the iScript cDNA Synthesis Kit.

2.3.3 PCR Validation

The cDNA extracted from the *Nicotiana benthamiana* plants with expression of the VL3320 gene was used as a DNA template in a PCR with VL3320 primers in order to ensure the transient expression of the gene. Primers (table 4) for a housekeeping *Nicotiana benthamiana* 18S gene were also used.

2.3.4 Confocal Microscopy

The leaves of the plants infiltrated with the construct for the transient expression of VL3320pGWB506 with GFP as well as the free GFP construct were cut and placed on a microscope slide. The Zeiss confocal laser scanning microscopes LSM800 was used in order to identify the localisation of VL3320 *in planta*. The GFP was excited at 488 nm and signals were collected at 680–700 nm.

2.4 Transcription analysis of host immunity marker genes

The cDNA extracted from the infiltrated *Nicotiana benthamiana* plants was used in RT-qPCR with a 2-Step Melt Amp protocol to analyse changes in host immunity when VL3320 was transiently expressed in the plant for both timepoints. The housekeeping primers for the *Nicotiana benthamiana* 18S gene were used to normalise the results. The primers used were to identify if there was expression of pathogenesis related proteins involved in salicylic acid signalling and systemic acquired resistance (PR1 and PR2) and jasmonic acid (JA) signalling and local acquired resistance (PR4) (Ali *et al.*, 2018). Primers for WRKY genes were also

used as WRKY is involved in both HR and cell death in response to pathogen infection (WRKY7 [Adachi et al., 2016]) and resistance to pathogen infection (WRKY8 [(Yong-Feng et al., 2019)]. PTI5 activates defence responses (Gu et al., 2002) HIN1 triggers defence responses after biotic stress (Zhang et al., 2022) and MAPKKKa is a regulator of PCD (Del Pozo, Pedley and Martin, 2004).

Table 3. Primers used and respective candidate gene targets in qPCR for the identification of PR protein expression in transformed *Nicotiana benthamiana*

Gene Target	Primer Name	Primer Sequence 5' – 3'
18S Ribosome	Nb18S-F	ATACGTGCAACAAACCCCGAC
18S Ribosome	Nb18S-R	TGAATCATCGCAGCAACGG
PTI5	qNbPti5-F	CCTCCAAGTTTGGAGCTCGGATAGT
PTI5	qNbPti5-R	CCAAGAAATTCTCCATGCACTCTGTGTC
WRKY7	qNbWRKY7-F	CACAAGGGTACAAACAACACAG
WRKY7	qNbWRKY7-R	GGTTGCATTTGGTTCATGTAAG
WRKY8	qNbWRKY8-F	AACAATGGTGCCAATAATGC
WRKY8	qNbWRKY8-R	TGCATATCCTGAGAAACCATT
PR4	qNbPR4-F	GGCCAAGATTCCTGTGGTAGAT
PR4	qNbPR4-R	CACTGTTGTTTGGAGTTCCTGTTCCCT
HIN1	qNbHIN1-F	CCAACCTGAACGGAGCCTATTA
HIN1	qNbHIN1-R	AGGCATCCAAAGAGACAACACTAC
PR1	qNbPR1a-F	CCGCCTTCCCTCAACTCAAC
PR1	qNbPR1a-R	GCACAACCAAGACGTACTIONGAG
PR2	qNbPR2-F	AGGTGTTTGGCTATGGAATGC
PR2	qNbPR2-R	TCTGTACCCACCATCTTGC
NbMAPKKKa	NbMAPKKa-F	GGTTGTTTTGGGATGTGGGGTCAG
NbMAPKKKa	NbMAPKKa-R	CAGTGGGCTCAACCTATTATCGCC

2.5 Hypersensitive Response Induction

The purified VL3320 in the binary vector pgWB602, empty vector pgWB602, Avr4, and ΔCD were grown in 25ml of LB media for 2 days at 28°C in a shaker. The resuspended cells in the tube were then centrifuged at 3500rpm for 10 minutes at 21°C and the solute was discarded. The pellet was then dissolved in induction buffer containing 0.5M MES buffer (final concentration 10mM), 100mM acetosyringone (final concentration 150μM), 1M MgCl₂ (final concentration 10mM), and distilled water up to 100ml. This was then repeated, and the

suspensions were then incubated in 28°C for two hours in a shaker. After two hours, the OD of the cells was diluted to 0.5, apart from Avr4 which was diluted to 0.03 OD.

The suspensions were transformed into 2-week-old *Nicotiana benthamiana* plants by syringe infiltration on the abaxial side of the leaf. 8 plants were used and two leaves were infiltrated on each plant. Each leaf was infiltrated with the VL3320pgBW602, empty binary vector PGWB602 and Δ CD suspensions produced in the aforementioned method, with one infiltration only being the induction buffer as a control, resulting in 4 infiltrations on each leaf, 2 on each side of the midrib. The infiltrated area was outlined with a marker. The plants were grown overnight and then the areas infiltrated with the empty vector, induction buffer and Δ CD were infiltrated again with the Avr4 suspension in order to induce the hypersensitive response (Postma *et al.*, 2016).

3. Results

3.1 Genome Analysis and Phylogeny of Peptidase Inhibitors

The presence of the peptidase inhibitor I78 domain was first identified using the SMART software as shown in figure 9. This protein also contains a signal peptide at the N- terminus, indicating targeting to the Endoplasmic Reticulum.

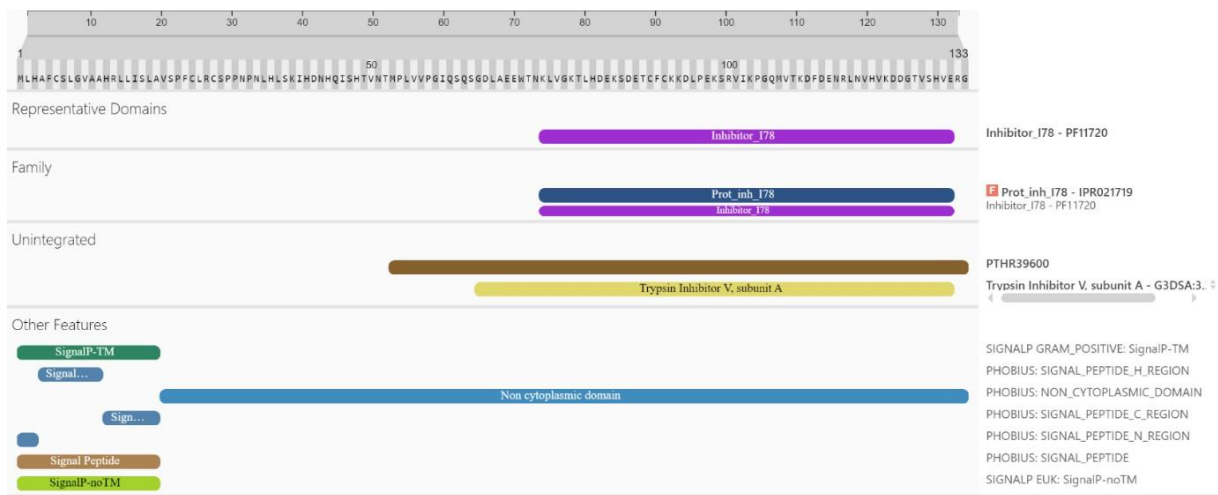


Figure. 9: SMART analysis results identifying the presence of the inhibitor I78 from analysis of the VL3320 gene

In the phylogeny (figure 10) it is apparent that homologs of the VL3320 gene may be conserved throughout the family of fungi, as well as in some species of bacteria: the gram-negative *Rhodospirillum rubrum* and *Vitreimonas* sp., a genus of Pseudomonadota. Each species listed here contains the I78 peptidase inhibitor domain and therefore it is possible to assume that they have similar function to our target gene VL3320.

The phylogeny shows that the *Verticillium* I78 peptidase inhibitors are closely related to homologs from *N. haematococca*, and *Fusarium sulawusience* although the node support was relatively low (figure 10).

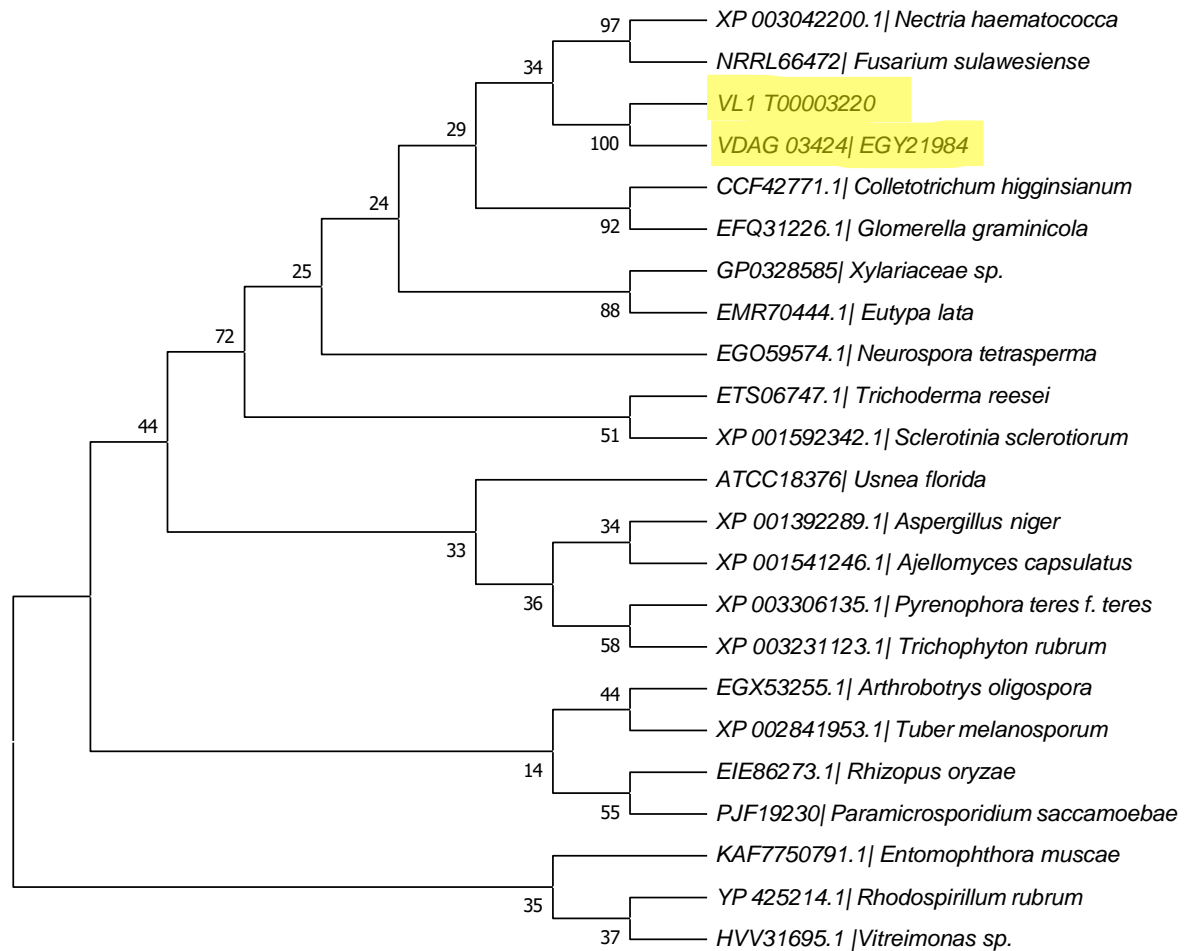


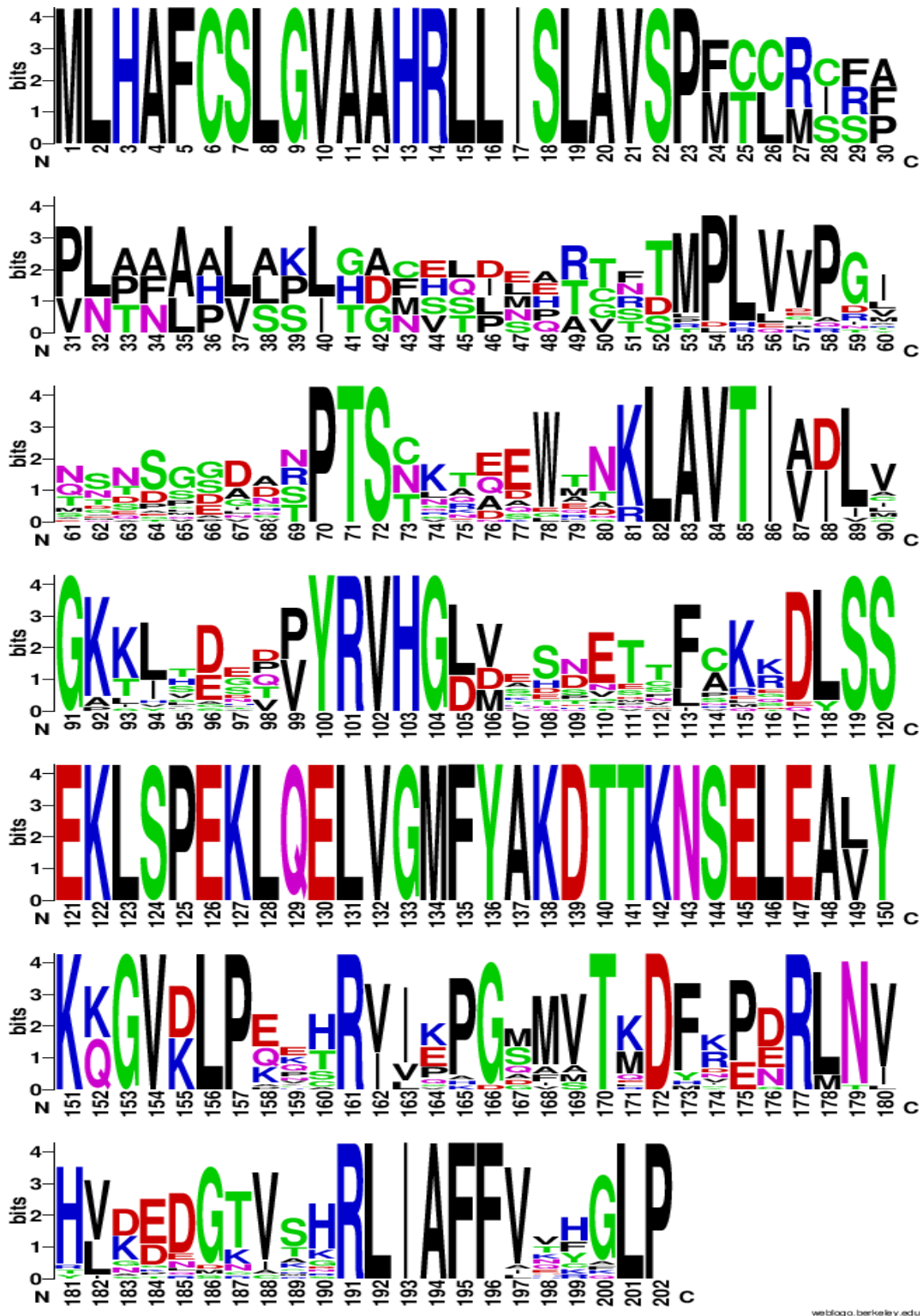
Figure. 10: Molecular Phylogenetic analysis of genes found by MycoCosm with the I78 peptidase inhibitor present using the Maximum Likelihood method based on Whelan and Goldman model. Highlighted genes denote the genes of interest analysed from *V. longisporum* and *V. dahlia*.

Table 4: Analysis of taxonomic groups where the I78 peptidase inhibitor was present after blasting the VL3320 gene against them using MycoCosm.

	Hits	Peptidase inhibitor present?
Pucciniomycotina	0	No
Ustilaginomycotina	0	No
Agaricomycetes	9	No
Dacrymycetes	0	No
Tremellomycetes	0	No
Wallemiomycetes	0	No
Pezizomycetes	761	Yes
Orbiliomycetes	1	Yes
Eurotiomycetes	1593	Yes
Dothideomycetes	1705	Yes
Lecanoromycetes	6	No
Leotiomycetes	559	Yes
Sordariomycetes	3460	Yes
Xylonomycetes	2	No

Saccharomycotina	102	Yes
Taphrinomycotina	10	Yes
Glomeromycotina	2	Yes
Mortierellomycotina	0	No
Mucoromycotina	122	Yes
Zoopagomycotina	11	Yes
Entomophthoromycotina	27	Yes
Kickxellomycotina	3	No
Blastocladiomycota	59	Yes
Chytridiomycetes	0	No
Monoblepharidomycetes	0	No
Neocallimastigomycetes	0	No
Microsporidia	0	No
Cryptomycota	1	Yes

In table 4, the I78 peptidase inhibitor is present in 11 out of 28 taxonomic groups, with its highest occurrence of 3460 unsurprisingly being in Sordariomycota. The peptidase inhibitor is not present in any taxonomic groups within basidiomycota (Pucciniomycotina, Ustilaginomycotina, Agaricomycetes, Dacrymycetes, Tremellomycetes, Wallemiomycetes), but is present in groups within Mucoromycota, Zoopagomycota, Chytridiomycota, and Cryptomycota.



weblogo.berkeley.edu

Fig. 11: A sequence logo denoting the sequence conservation of the homologs containing the 178 peptidase inhibitor region of VL3320. Made using WebLogo (Crooks et al., 2004) Each logo consists of stacks of symbols, one stack for each position in the sequence. The overall height of the stack indicates the sequence conservation at that position, while the height of symbols within the stack indicates the relative frequency of each amino acid at that position.

The signal peptide and sequence in the middle region spanning from 119 to 148 bases appears to be highly conserved among all the homologs analysed in the phylogenetic tree, alluding to it being the catalytic domain as also shown in figure 9.

3.2 Gene Expression Analysis of VL3320 and VD3424 *in planta*

In analysing the gene expression of both the VD3424 and VL3320 genes (figure 12), the highest transcription of the gene can be seen around 4-6 days post infection. In VD3424, the expression of the gene is highest at 5 days post infection and begins to decrease similarly to VL3320 until 8 days post infection where it increases again, albeit not as highly as 5 days post infection. In VL3320, the gene expression increases steadily from the initial infection to 6 days post infection, before significantly decreasing to levels lower than mycelial at 8- and 10-days post infection. This significant decrease suggests that the target gene is involved in initial infection and the period of hyphal proliferation and conidia production, wherein the conidia germinate and colonize the vascular elements upstream of the stem.

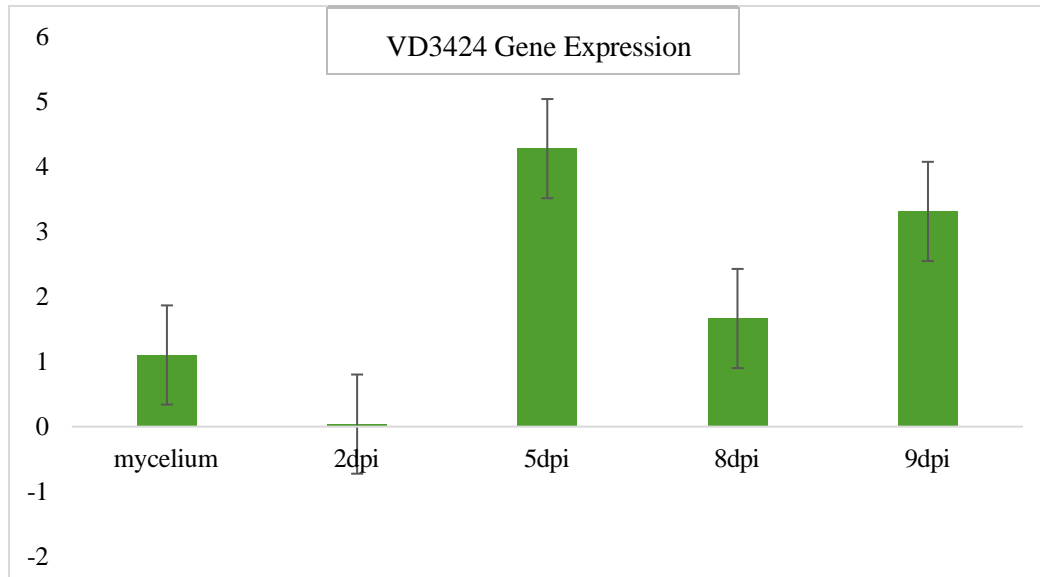


Fig. 12: Gene expression of VD3424 in *Solanum lycopersicum* variety 'Moneymaker' at mycelial stage, 2, 5, 8, and 9 days post infection with *Verticillium dahliae* isolate JR2.

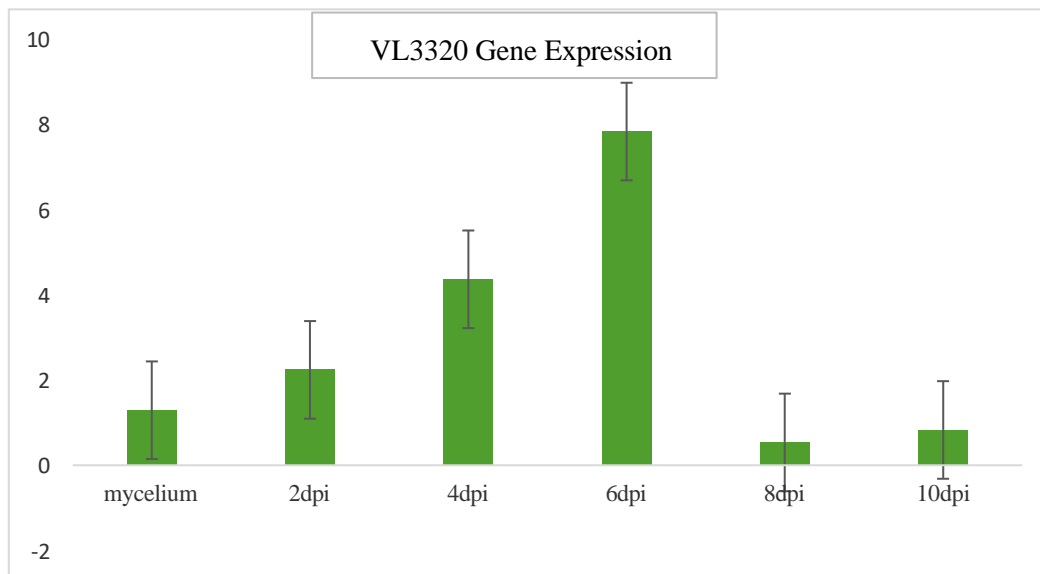


Fig. 13: Gene expression of VL3320 in *Brassica napus* variety 'Hannah' at mycelial stage, 2, 4, 6, 8 and 10 days post infection with *Verticillium longisporum* isolate VL-1.

3.3 Construction of *V. dahliae* deletion strain

The protoplast transformation containing the VD3424 deletion cassette did not produce any positive colonies although repeated twice. The binary vector used therefore may not have been ideal for plant transformation due to incompatible forward and reverse borders present in the initial vector. The death controls unexpectedly gave colonies and therefore there may have been an issue with the concentration of antibiotic or with the protoplast transformation itself.

3.4 VL3320 Transient Expression in plants

3.4.1 Confocal Microscopy of 506 Construct and Free GFP Construct

The construct with the expression of free GFP showed constitutive expression of GFP within the area of the leaf that had been infiltrated. The leaves agroinfiltrated with the VL3320 gene however did not show any GFP expression and therefore it was not possible to determine the localisation of VL3320 in the plant cells at 72hpi (figure 14), indicating that possible RNA silencing mechanisms had been activated by the plant, upon transient expression of this gene.

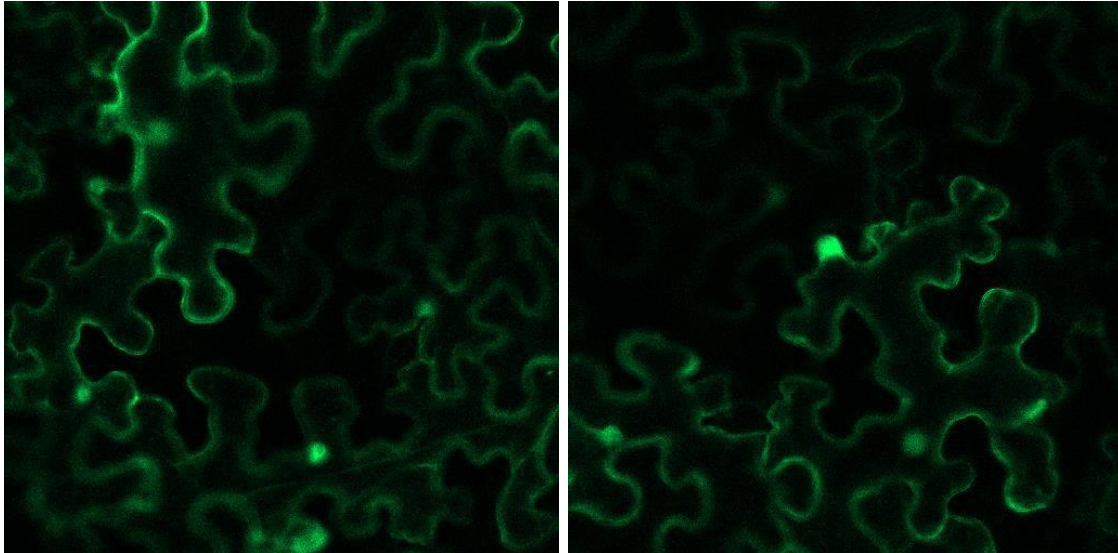


Fig. 14: Zeiss confocal laser scanning microscope LSM800 showing microscopy of leaf expressing free GFP construct in *Nicotiana benthamiana*

3.4.2 Gene Expression Analysis of in *Nicotiana benthamiana*

The primers were used to identify if there was expression of pathogenesis related proteins involved in salicylic acid signalling and systemic acquired resistance (PR1 and PR2) and jasmonic acid signalling and local acquired resistance (PR4) (Ali *et al.*, 2018). Primers for WRKY genes were also used as WRKY is involved in both HR and cell death in response to pathogen infection (WRKY7), (Adachi *et al.*, 2016), and resistance to pathogen infection (WRKY8), (Yong-Feng *et al.*, 2019). PTI5 activates defence responses and activates the expression of PR1 and PR2 (Gu *et al.*, 2002) HIN1 is involved in defence responses after pathogen infection and abiotic stress, and leaf senescence (Takahashi *et al.*, 2004, Zhang *et al.*, 2022) and MAPKKKa is a regulator of programmed cell death (PCD) (Del Pozo, Pedley and Martin, 2004).

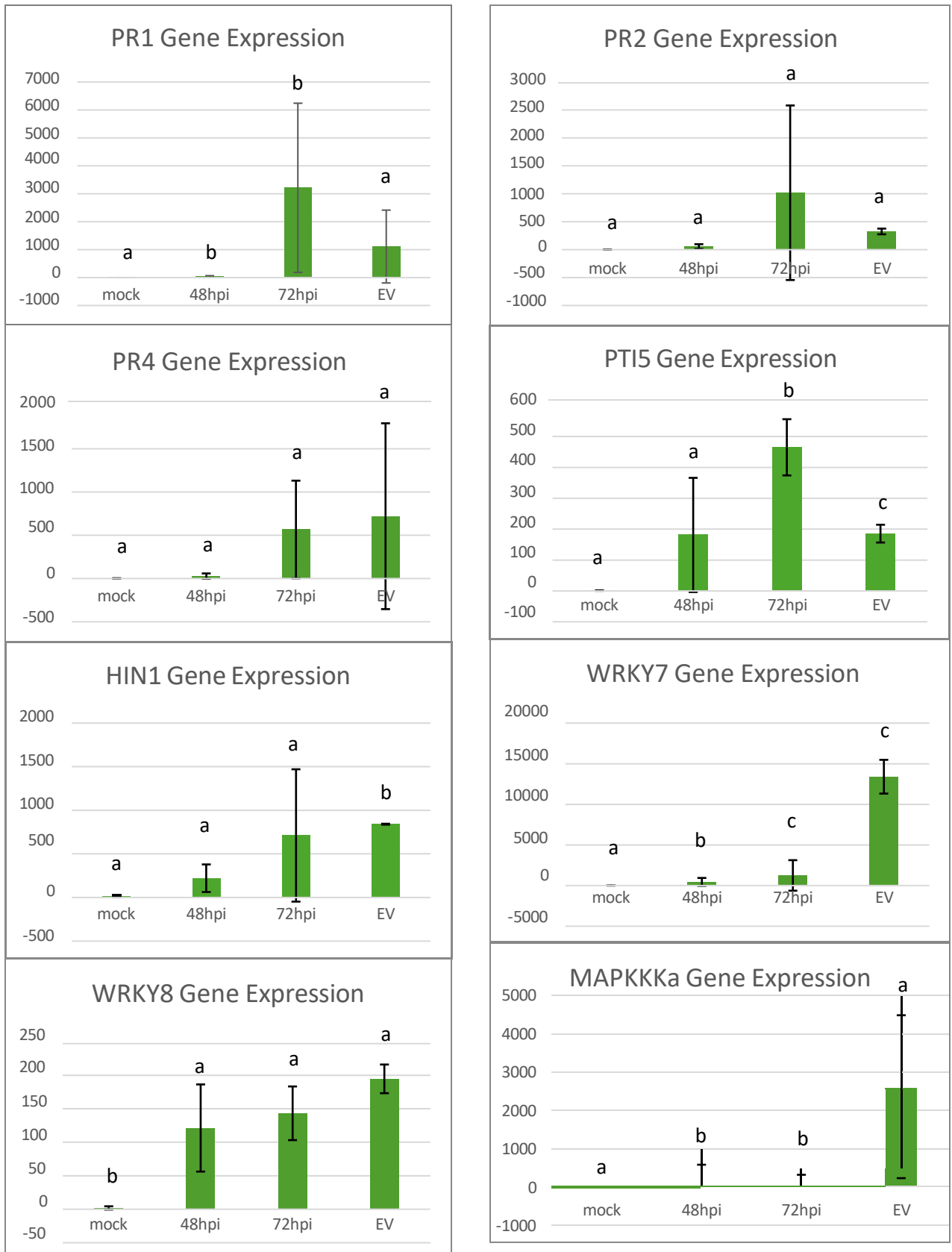


Fig. 15: Graphs detailing the gene expression. Y axis denotes to the RT-qPCR Ct values normalised against *Nicotiana benthamiana* 18S gene expression after infecting with VL3320pgWB602. Corresponding letters denote no significant difference between each other (p -value >0.05) while differing letters corresponds to a significant difference (p -value: ≤ 0.05)

4. Discussion

4.1 Gene Expression of VD3424 and VL3320

In the infection of tomato variety ‘Moneymaker’ with the *V. dahliae* strain JR2, the expression of VD3424 was highest at 5 days post infection before decreasing. Similarly, the infection of the rapeseed variety ‘Hannah’ with the *V. longisporum* strain VL1 showed the highest levels of gene expression at 5 days post infection before decreasing. This result alludes to the involvement of VD3424 and VL3320 in infection, due to their increased expression.

4.2 Transient Expression of VL3320

Analysis of the RT-qPCR results show that the transient expression of *VL3320* induces a defence response from the host and causes a significant upregulation of the PR proteins and transcription factor *PR1*, *PTI5*, and *WRKY7*. Conversely, there appears to be a suppression of *HIN1* and *MAPKKKa*, and further analysis could determine whether *VL3320* is able to suppress proteins or transcription factors involved in the hypersensitive response and programmed cell death molecular pathways.

PR1 is highly abundant in several plants, and downstream defence responses are activated by the production and activation of the CAPE1 peptide in the apoplastic space by PR1 (Han *et al.*, 2023). Several studies suggest that PR1 is involved in the recruitment of TLPs (thaumatin-like proteins) in the PR5 family and LTPs (lipid transfer proteins) like PR14 involved in plant defence responses (Han *et al.*, 2023). Several fungal species such as *Fusarium oxysporum* attenuate the defence capabilities of PR1 by translocating PR1 from the apoplastic space into the host cell nucleus using the fungal effector FolSvp1, where the CAPE1 signalling peptide is therefore not able to be generated or activated (Li *et al.*, 2022). Based on the significantly upregulated expression of PR1 (figure 15), *VL3320* is not able to suppress the apoplastic activity of PR1, and it can therefore be assumed that the activity of the PR5 family and PR14 TLPs are induced downstream of the induction of PR1 by *VL3320*.

The significant upregulation (p-value: 0.038) of PR1 at the second time point as compared to the first time point suggests that the transient expression of *VL3320* possibly causes an induction of salicylic acid (SA) and activation of plant immune signalling after 72 hours (figure

15). It is therefore possible to assume that further downstream targets of SA are also induced such as the production of reactive oxygen species (ROS) (Mishra *et al.*, 2024). PR2 shows no significant differences between any of the time points or controls and we can therefore assume that PR2 is not up or downregulated in response to VL3320.

PR4 is another pathogenesis related protein, involved instead in JA synthesis and local acquired resistance. JA-regulated local acquired resistance is often associated with wounding from herbivore damage and rhizobacterial colonisation (Ruan *et al.*, 2019). PR4 is not significantly upregulated in any plants, and from the data presented we can therefore assume that VL3320 does not induce jasmonic acid regulated immunity.

PTI5 activates downstream reporter GCC-box transcription factors, and in *Arabidopsis* it has been noted that activation of PTI5 is able to enhance the expression of PR1 and PR2 and therefore induce other SA-mediated defence genes. Due to its upregulation in response to the expression of VL3320, it is plausible to assume these genes are also upregulated. PTI5 is involved in defence and is an activator of the PR proteins PR1 and PR2, and therefore the upregulation of PTI5 is expected and seen in this experiment to be consistent with results seen from PR1, with a significant difference between the second time point and mock (p-value: 0.0032), the first time point (p-value: 0.037), and EV (p-value: 0.005). From this data it appears that the VL3320 gene is involved in the activation of PTI5, further bolstered by the upregulation seen in PR1.

WRKY7 is a transcriptional repressor of SA mediated signalling. It is expected that the expression of WRKY7 would be opposite to the expression levels in SA-signalling involved genes such as *PR1*. Due to the result seen (figure 15) as well as the significantly high standard deviation (SD second time point: 1880; SD EV: 2078), the experiment should be repeated. In WRKY7, the expression values of EV are significantly higher than any of the other plants. WRKY7 is involved in both HR and cell death in response to pathogen infection, and its significantly low expression in VL3320-transiently expressed plants harvested at both the first and second timepoint could potentially suggest that the VL3320 gene is able to suppress the induction of WRKY8 and potentially HR.

WRKY8 is phosphorylated by MAPK to induce the expression of defence related genes and is significantly upregulated in both the first (0.015) and second time point (and the EV plants compared the mock). This may suggest that wounding from the initial syringe infiltration upregulated WRKY8, as it is generally induced by wounding (Chen, Zhang and Yu, 2010).

HIN1 is a gene induced by the presence of hairpins and is involved in the elicitation of HR, with rapid increases in expression after induction by *avrPto*-mediated HR in tomato (Gopalan, Wei and He, 1996). HIN1 has uncharacterised molecular patterns but is generally assumed to behave in an unspecific pathogen defence related pathway (Ciccarelli and Bork, 2004). As well as its involvement in HR, HIN1 is also significantly upregulated and involved in drought acclimation and water stress pathways (Chong *et al.*, 2019), and is dephosphorylated by HAI1 in drought conditions. It is involved in splicing and regulating the expression of stress related proteins such as NAC062, involved in both abiotic stress and pathogen resistance (Chong *et*

al., 2019). HIN1 is a gene involved in the induction of plant defence and may be involved in the induction of HR based on studies surrounding its involvement in leaf senescence (Takahashi et al., 2004). Due to its significant downregulation in plants expressing *VL3320*, it is plausible to assume that *VL3320* interacts with HIN1 or other genes in HR-signalling pathways in order to inhibit HR. It is significantly upregulated in the EV (p-value: <0.05) plants. This may suggest that *VL3320* is able to suppress HIN1, however the standard deviation in the results of the second time point require the experiment to be repeated to provide identifiable information on the interaction between HIN1 and *VL3320* (standard deviation: 758.73).

MAPKKKa is a gene with significant regulatory roles in plant cell death. If MAPKKKa is silenced, plant cell death does not occur (Del Pozo, Pedley and Martin, 2004). Two MAPKK signalling cascades are induced upon the expression of MAPKKKa - MEK1/NTF6, as a regulator of HR in incompatible pathogen interactions. In compatible pathogen interactions, MAPKKKa induces plant cell death (Del Pozo, Pedley and Martin, 2004). In the expression results, it is clear that MAPKKKa is silenced or significantly downregulated in response to infection with *VL3320*. As MAPKKKa is induced naturally both in incompatible and compatible pathogen interactions, if *VL3320* did not interact with MAPKKKa there would still be upregulation visible in the results. Therefore, the suppression of MAPKKKa by *VL3320* is something that should be further explored through testing *VL3320s* capability to suppress HR. MAPKKKa is involved in cell death and regulates plant cell death. Similarly to the results seen in WRKY7, the 2-ddCT is significantly higher in EV than other data points (p-value: 0.037641975) and could be due to *VL3320* being able to suppress cell death.

In order to determine if and how *VL3320* is able to suppress cell death responses, further Rt-qPCRs using primers for genes involved in HR such as *NtErf3*, a positive regulator of plant cell death (Noman et al., 2020) should be performed. Several 2-ddCT values showed significant levels of variation, producing a high standard deviation and therefore meant that several results did not show significant differences between the mock, EV or pGWB602*VL3320* infiltrated plants.

4.3 Gene Deletion of VD3424

The protoplast transformation unfortunately did not produce the expected colonies, and after repeating the experiment the same results were observed. In the future, the application of a more recent genetic transformation method of *Agrobacterium*-mediated genetic transformation used previously on Shine Muscat grape or another method which integrates the CRISPR/Cas9 system in *Agrobacterium*-mediated and embryogenic callus induction may instead be deployed (Wang *et al.*, 2023, Li *et al.*, 2022). Another method used successfully several times for the deletion of *V. dahliae* genes known as the OSCAR method may also be

used, which follows a similar protocol while the marker and assembly vector are changed (Gold et al., 2017). However, the vector used is not compatible with agro-transformation due to the forward border and backwards border, and a new deletion vector must be designed.

4.3.1 Subcellular Localisation of pgWB506VL3320

The transient expression cassette may not have worked due to the OD being too low, or that the acidity in the intracellular space being too high. As GFP is inactivated by high acidity, and the *VL3320* gene is proposed to be secreted intracellularly, the reason for the lack of GFP fluorescence when analysing the localisation of the *VL3320* protein may be due to the acidity. In the future, another fluorescent tag may be used instead such as mCherry (pKa = 3.8), or the OD adjusted to be higher than 0.2. In many cases, the GFP itself can interfere with the protein and therefore disrupt function due to its placement on either the N- or C- terminus during post-translation modification, instead the GFP tag may be placed into the coding area of the *VL3320* gene to avoid misregulated folding of the gene (Adjobo-Hermans et al., 2011).

5. Conclusion

To conclude, *VL3320* interacts with several genes involved in plant immunity, and is upregulated significantly during *Verticillium* infection, suggesting that it has a role in virulence. These results suggest that the role of peptidase inhibitors in *Verticillium* infection is prominent during the stage of colonisation rather than the initial infection. In order to fully identify the role of *VL3320*, new techniques for the study of amphidiploid fungal genomes are required in order to understand the importance and role of *VL3320* in infection. The identification of virulence genes as well as a broader understanding of amphidiploid fungal genomes will allow research to be tailored towards the production of R genes in target hosts and is of fundamental importance in the wider economic landscape and sustainable production of food.

References

Adachi, H. et al. (2016) '*Nicotiana benthamiana* MAPK-WRKY pathway confers resistance to a necrotrophic pathogen *Botrytis cinerea*,' *Plant Signalling & Behavior/Plant Signalling & Behaviour*, 11(6), p. e1183085. <https://doi.org/10.1080/15592324.2016.1183085>.

Adjobo-Hermans, M.J. et al. (2011) 'Real-time visualization of heterotrimeric G protein Gq activation in living cells,' *BMC Biology*, 9(1). <https://doi.org/10.1186/1741-7007-9-32>.

Ali, S. et al. (2018) 'Pathogenesis-related proteins and peptides as promising tools for engineering plants with multiple stress tolerance,' *Microbiological Research*, 212–213, pp. 29–37. <https://doi.org/10.1016/j.micres.2018.04.008>.

Chen, L., Zhang, L. and Yu, D. (2010) 'Wounding-Induced WRKY8 is involved in basal defense in Arabidopsis,' *Molecular Plant-microbe Interactions*, 23(5), pp. 558–565. <https://doi.org/10.1094/mpmi-23-5-0558>.

Chong, G.L. et al. (2019) 'Highly ABA-Induced 1 (HAI1)-Interacting protein HIN1 and drought acclimation-enhanced splicing efficiency at intron retention sites,' *Proceedings of the National Academy of Sciences of the United States of America*, 116(44), pp. 22376–22385. <https://doi.org/10.1073/pnas.1906244116>.

Ciccarelli, F.D. and Bork, P. (2004) 'The WHY domain mediates the response to desiccation in plants and bacteria,' *Bioinformatics*, 21(8), pp. 1304–1307. <https://doi.org/10.1093/bioinformatics/bti221>.

Crooks, G.E. et al. (2004) 'WebLogo: A Sequence Logo Generator,' *Genome Research*, 14(6), pp. 1188–1190. <https://doi.org/10.1101/gr.849004>.

Depotter, J.R.L. et al. (2017) 'A distinct and genetically diverse lineage of the hybrid fungal pathogen *Verticillium longisporum* population causes stem striping in British oilseed rape,' *Environmental Microbiology*, 19(10), pp. 3997–4009. <https://doi.org/10.1111/1462-2920.13801>.

Del Pozo, O., Pedley, K.F. and Martin, G.B. (2004) 'MAPKKK α is a positive regulator of cell death associated with both plant immunity and disease,' *EMBO Journal*, 23(15), pp. 3072–3082. <https://doi.org/10.1038/sj.emboj.7600283>.

Depotter, J.R.L. *et al.* (2016) 'Verticillium longisporum, the invisible threat to oilseed rape and other brassicaceous plant hosts,' *Molecular Plant Pathology*, 17(7), pp. 1004–1016. <https://doi.org/10.1111/mpp.12350>.

Dunaevsky, Y.E. *et al.* (2014) 'Fungal inhibitors of proteolytic enzymes: Classification, properties, possible biological roles, and perspectives for practical use,' *Biochimie*, 101, pp. 10–20. <https://doi.org/10.1016/j.biochi.2013.12.007>.

Fradin, E.F. and Thomma, B.P.H.J. (2006) 'Physiology and molecular aspects of Verticillium wilt diseases caused by *V. dahliae* and *V. albo-atrum*,' *Molecular Plant Pathology*, 7(2), pp. 71–86. <https://doi.org/10.1111/j.1364-3703.2006.00323.x>.

Gold, S.E. *et al.* (2017) 'Rapid Deletion Production in Fungi via *Agrobacterium*-Mediated Transformation of OSCAR Deletion Constructs,' *Journal of Visualized Experiments* [Preprint], (124). <https://doi.org/10.3791/55239>.

Gopalan, S., Wei, W. and He, S.Y. (1996) 'hrp gene-dependent induction of hin1: a plant gene activated rapidly by both harpins and the avrPto gene-mediated signal,' *Plant Journal*, 10(4), pp. 591–600. <https://doi.org/10.1046/j.1365-313x.1996.10040591.x>.

Gu, Y. *et al.* (2002) 'Tomato transcription factors PTI4, PTI5, and PTI6 activate defense responses when expressed in *Arabidopsis*,' *The Plant Cell*, 14(4), pp. 817–831. <https://doi.org/10.1105/tpc.000794>.

Han, Z. *et al.* (2023) 'The function of plant PR1 and other members of the CAP protein superfamily in plant–pathogen interactions,' *Molecular Plant Pathology*, 24(6), pp. 651–668. <https://doi.org/10.1111/mpp.13320>.

Hanada, K. *et al.* (1978) 'Isolation and characterization of E-64, a new thiol protease inhibitor.,' *Agricultural and Biological Chemistry*, 42(3), pp. 523–528. <https://doi.org/10.1271/bbb1961.42.523>.

Heale, J.B. and Karapapa, V.K. (1999) 'The verticillium threat to Canada's major oilseed crop: canola,' *Canadian Journal of Plant Pathology*, 21(1), pp. 1–7. <https://doi.org/10.1080/07060661.1999.10600114>.

Karapapa, V.K., Bainbridge, B.W. and Heale, J.B. (1997) 'Morphological and molecular characterization of *Verticillium longisporum* comb. Nov., pathogenic to oilseed rape,' *Mycological Research*, 101(11), pp. 1281–1294. <https://doi.org/10.1017/s0953756297003985>.

Kumar, S., Stecher, G. and Tamura, K. (2016) 'MEGA7: Molecular Evolutionary Genetics Analysis Version 7.0 for bigger datasets,' *Molecular Biology and Evolution*, 33(7), pp. 1870–1874. <https://doi.org/10.1093/molbev/msw054>.

Li, J. *et al.* (2022) 'Acetylation of a fungal effector that translocates host PR1 facilitates virulence,' *eLife*, 11. <https://doi.org/10.7554/elife.82628>.

Li, M. et al. (2022) '*Agrobacterium*-Mediated genetic transformation of embryogenic callus in a liriiodendron hybrid (*L. chinense* × *L. tulipifera*),' *Frontiers in Plant Science*, 13. <https://doi.org/10.3389/fpls.2022.802128>.

Lo Presti, L. et al. (2015) 'Fungal effectors and plant susceptibility,' *Annual Review of Plant Biology*, 66(1), pp. 513–545. <https://doi.org/10.1146/annurev-arplant-043014-114623>.

Mehrabi, R. et al. (2015) 'Flexible gateway constructs for functional analyses of genes in plant pathogenic fungi,' *Fungal Genetics and Biology*, 79, pp. 186–192. <https://doi.org/10.1016/j.fgb.2015.03.016>.

Mishra, S. et al. (2024) 'Salicylic acid (SA)-mediated plant immunity against biotic stresses: an insight on molecular components and signalling mechanism,' *Plant Stress*, 11, p. 100427. <https://doi.org/10.1016/j.stress.2024.100427>.

Nakagawa, T. et al. (2007) 'Development of series of gateway binary vectors, pGWBs, for realizing efficient construction of fusion genes for plant transformation,' *Journal of Bioscience and Bioengineering*, 104(1), pp. 34–41. <https://doi.org/10.1263/jbb.104.34>.

Njoroge, S.M.C. et al. (2011) 'Phenological and Phytochemical Changes Correlate with Differential Interactions of *Verticillium dahlia* with Broccoli and Cauliflower,' *Phytopathology*, 101(5), pp. 523–534. <https://doi.org/10.1094/phyto-08-10-0219>.

Novakazi, F. et al. (2015) 'The Three Lineages of the Diploid Hybrid *Verticillium longisporum* Differ in Virulence and Pathogenicity,' *Phytopathology*, 105(5), pp. 662–673. <https://doi.org/10.1094/phyto-10-14-0265-r>.

Postma, J. et al. (2016) 'Avr4 promotes Cf-4 receptor-like protein association with the BAK1/SERK3 receptor-like kinase to initiate receptor endocytosis and plant immunity,' *New Phytologist*, 210(2), pp. 627–642. <https://doi.org/10.1111/nph.13802>.

Rafiei, V. et al. (2022) 'Investigating the role of a putative endolysin-like candidate effector protein in *Verticillium longisporum* virulence,' *Biochemical and Biophysical Research Communications*, 629, pp. 6–11. <https://doi.org/10.1016/j.bbrc.2022.08.086>.

Ruan, J. et al. (2019) 'Jasmonic acid signalling pathway in plants,' *International Journal of Molecular Sciences*, 20(10), p. 2479. <https://doi.org/10.3390/ijms20102479>.

Sabotič, J. and Kos, J. (2012) 'Microbial and fungal protease inhibitors—current and potential applications,' *Applied Microbiology and Biotechnology*, 93(4), pp. 1351–1375. <https://doi.org/10.1007/s00253-011-3834-x>.

Sharma, P. and Gayen, D. (2021) 'Plant protease as regulator and signaling molecule for enhancing environmental stress-tolerance,' *Plant Cell Reports*, 40(11), pp. 2081–2095. <https://doi.org/10.1007/s00299-021-02739-9>.

Shi-Kunne, X. et al. (2019) 'The genome of the fungal Pathogen *Verticillium dahliae* reveals extensive bacterial to fungal gene transfer,' *Genome Biology and Evolution*, 11(3), pp. 855–868. <https://doi.org/10.1093/gbe/evz040>.

Song, Y. and Thomma, B.P.H.J. (2016) 'Host-induced gene silencing compromises *Verticillium* wilt in tomato and Arabidopsis,' *Molecular Plant Pathology*, 19(1), pp. 77–89. <https://doi.org/10.1111/mpp.12500>.

Takahashi, Y. et al. (2004) 'Identification of Tobacco HIN1 and Two Closely Related Genes as Spermine-Responsive Genes and their Differential Expression During the Tobacco Mosaic Virus-Induced Hypersensitive Response and During Leaf- and Flower-Senescence,' *Plant Molecular Biology*, 54(4), pp. 613–622. <https://doi.org/10.1023/b:plan.0000038276.95539.39>.

Tanaka, S. et al. (2014) 'A secreted *Ustilago maydis* effector promotes virulence by targeting anthocyanin biosynthesis in maize,' *eLife*, 3. <https://doi.org/10.7554/elife.01355>.

Trapero, C. et al. (2013) 'Effective inoculation methods to screen for resistance to *Verticillium* wilt in olive,' *Scientia Horticulturae*, 162, pp. 252–259. <https://doi.org/10.1016/j.scienta.2013.08.036>.

Tzelepis, G. et al. (2017) 'Detection of *Verticillium* species in Swedish soils using real-time PCR,' *Archives of Microbiology*, 199(10), pp. 1383–1389. <https://doi.org/10.1007/s00203-017-1412-z>.

Vega-Marin, M. and Von Tiedemann, A. (2023) 'Contrasting interactions of the aggressive *Verticillium longisporum* lineage A1/D1 and the non-aggressive A1/D2 lineage with roots of oilseed rape,' *Plant Pathology*, 72(9), pp. 1662–1672. <https://doi.org/10.1111/ppa.13787>.

Wang, S. et al. (2023) '*Agrobacterium tumefaciens*-mediated transformation of embryogenic callus and CRISPR/Cas9-mediated genome editing in 'Feizixiao' litchi,' *Horticultural Plant Journal*, 9(5), pp. 947–957. <https://doi.org/10.1016/j.hpj.2023.01.011>.

Whelan, S. and Goldman, N. (2001) 'A General Empirical Model of Protein Evolution Derived from Multiple Protein Families Using a Maximum-Likelihood Approach,' *Molecular Biology and Evolution*, 18(5), pp. 691–699. <https://doi.org/10.1093/oxfordjournals.molbev.a003851>.

Zhang, D. et al. (2022) 'The secretome of *Verticillium dahliae* in collusion with plant defence responses modulates *Verticillium* wilt symptoms,' *Biological Reviews*, 97(5), pp. 1810–1822. <https://doi.org/10.1111/brv.12863>.

Zhang, X. et al. (2022) 'Genome-wide identification and characterization of NHL gene family in response to alkaline stress, ABA and MEJA treatments in wild soybean (*Glycine soja*),' *PeerJ*, 10, p. e14451. <https://doi.org/10.7717/peerj.14451>.

Zheng, X. *et al.* (2019) 'Potential for Seed Transmission of *Verticillium longisporum* in Oilseed Rape (*Brassica napus*),' *Plant Disease*, 103(8), pp. 1843–1849. <https://doi.org/10.1094/pdis-11-18-2024-re>.

Zipfel, C. (2008) 'Pattern-recognition receptors in plant innate immunity,' *Current Opinion in Immunology*, 20(1), pp. 10–16. <https://doi.org/10.1016/j.coi.2007.11.003>.

Approved students' theses at SLU are published electronically. As a student, you have the copyright to your own work and need to approve the electronic publishing. If you check the box for YES, the full text (pdf file) and metadata will be visible and searchable online. If you check the box for NO, only the metadata and the abstract will be visible and searchable online. Nevertheless, when the document is uploaded it will still be archived as a digital file. If you are more than one author, the checked box will be applied to all authors. You will find a link to SLU's publishing agreement here:

- <https://libanswers.slu.se/en/faq/228318>.

YES, I/we hereby give permission to publish the present thesis in accordance with the SLU agreement regarding the transfer of the right to publish a work.

NO, I/we do not give permission to publish the present work. The work will still be archived and its metadata and abstract will be visible and searchable.